

N62 - 13232

NASA TR R-87

NASA TR R-87

# **NATIONAL AERONAUTICS AND SPACE ADMINISTRATION**

---

**TECHNICAL REPORT  
R-87**

## **A STUDY OF THE POSITIONS AND VELOCITIES OF A SPACE STATION AND A FERRY VEHICLE DURING RENDEZVOUS AND RETURN**

**By JOHN M. EGGLESTON and HAROLD D. BECK**

**1961**

---

---

# **TECHNICAL REPORT R-87**

---

## **A STUDY OF THE POSITIONS AND VELOCITIES OF A SPACE STATION AND A FERRY VEHICLE DURING RENDEZVOUS AND RETURN**

**By JOHN M. EGGLESTON and HAROLD D. BECK**

**Langley Research Center  
Langley Field, Va.**

---

---

I

## TECHNICAL REPORT R-87

### A STUDY OF THE POSITIONS AND VELOCITIES OF A SPACE STATION AND A FERRY VEHICLE DURING RENDEZVOUS AND RETURN

By JOHN M. EGGLESTON and HAROLD D. BECK

#### SUMMARY

*A study is made of the families of nonthrusting ascent trajectories of a ferry vehicle during rendezvous with an orbiting body, referred to as a space station. It is shown that these trajectories may also be interpreted as descent trajectories of the ferry from the station to the earth. The rendezvous trajectories start at the end of the boost period (assumed to be 60 miles) and terminate at the station. The equations of motion are derived and results are shown for two typical orbits of the station: a 300-mile circular orbit and a 100- to 500-mile elliptical orbit. Trajectories are described in terms of a rotating coordinate system fixed in the station and launch conditions are tabulated in terms of nonrotating inertial coordinates.*

*Boundaries are given in terms of launch (at time of booster burnout) and rendezvous conditions for the example cases. The considerations used to calculate these boundaries and the significance of some of the trends are discussed.*

#### INTRODUCTION

In its essence the rendezvous problem may be formulated in terms of two vehicles, the space station and the ferry vehicle. The space station is in an established orbit. The ferry vehicle is to be launched from some point on the earth and placed in a trajectory which intersects the orbit of the space station at the same instant that the space station reaches this intersection point. An additional requirement, that the relative velocities of the two vehicles be zero at interception, may or may not be imposed. If such a requirement were imposed, the zero relative velocity would ordinarily be obtained just prior to interception by terminal thrust control. Although formulated in terms of the approach of the ferry to the station,

it is evident that the related problems such as that of ejection of the ferry or some other mass from the space station so that it arrives above a certain point on the earth and the interception of orbital bodies do not involve any essential difference with rendezvous as described herein.

One of the primary concerns associated with the rendezvous mission is that of achieving once-a-day rendezvous capability and still not spending a large percentage of the payload on fuel for expensive space maneuvers. (See ref. 1.) If the thrusting maneuvers are to be kept small, the station must be in a favorable position in its orbit at the time the ferry launch site passes through or is in the near vicinity of the plane of the orbit. The problem may be resolved into two parts: (1) placing the station into a desirable orbit so that a favorable position of the station near the ferry launch site occurs once a day and (2) extending the time during which the station is in a favorable position to allow for delays in ferry launch time.

The first of these problems has been studied in references 1 to 4. References 1 and 2 point out that, if the maximum latitude of the station is only slightly greater than the latitude of the ferry launch site, once-a-day out-of-plane launches may be made with only a slight reduction in mass ratio. References 3 and 4 point out that rendezvous-compatible orbits for the station may be obtained if the station period is integrally related to the rotational period of the earth.

One approach to the second part of the problem is to avoid restriction of the ascent trajectory of the ferry to a minimum-energy or Hohmann ellipse but to investigate the variations in the ferry trajectory and in the relative positions of the ferry and station at the time of launch because of variations in the launch conditions (velocity, flight-path

angle, and time). The restrictions that rendezvous must still be achieved and achieved at a reasonable cost in mass ratio are then boundary conditions of the problem. This paper is concerned with the variations in the trajectories and launch conditions which will lead to a successful rendezvous.

When the various rendezvous trajectories were considered, no attempt was made to eliminate those launch conditions which do not lend themselves to "safe-launch" trajectories or to the limitations of specific boosters, although such considerations should be taken into account for any specific rendezvous mission.

### SYMBOLS

Any consistent set of units may be used for the analysis presented herein. In the examples given, it is assumed that

$$g_e = 32.17 \text{ feet per second per second}$$

$$r_e = 3,960 \text{ statute miles}$$

$$1 \text{ statute mile} = 5,280 \text{ feet}$$

$$1 \text{ foot} = 0.3048 \text{ meter}$$

$A$	semimajor axis of elliptic orbit of space station
$C$	constant angular momentum per unit mass
$E$	total energy
$F_i$	generalized external forces (lift, drag, thrust)
$g$	acceleration due to gravity
$g_e$	gravitational constant at earth's surface
$h$	altitude above earth's surface
$\mathbf{i}, \mathbf{j}, \mathbf{k}$	unit vectors in direction of $X$ -, $Y$ -, and $Z$ -axes, respectively
$I_{sp}$	specific impulse
$L$	Lagrangian, defined as $T - U$
$m$	mass of ferry vehicle
$q_i$	generalized coordinates in Lagrangian operation, $i = 1, 2, 3$
$R$	distance from space station to ferry vehicle
$r$	radial distance measured from earth's center of gravity
$T_x, T_y, T_z$	components of vehicle thrust acting in $x$ -, $y$ -, and $z$ -directions, respectively
$T$	kinetic energy
$t$	time

$U$	potential energy
$\Delta V$	relative velocity of ferry with respect to station
$V$	total velocity of ferry vehicle as observed from center of earth
$V_r$	radial component of $V$
$V_t$	tangential component of $V$
$V_\theta$	component of $V_t$ parallel to plane of station orbit
$V_\zeta$	component of $V_t$ perpendicular to plane of station orbit
$\Delta W$	change in the ferry vehicle weight due to fuel expenditure
$W$	weight of ferry vehicle
$X, Y, Z$	axes system with center fixed in space station. The $Z$ -axis is perpendicular to plane of orbit, the $X$ - and $Y$ -axes lie in plane of orbit with $Y$ always pointing away from center of earth.
$x, y, z$	three orthogonal components of rectangular coordinate system
$\alpha$	angle measured from $X$ -axis to projection of relative velocity $\Delta V$ on the $x, y$ plane, $\tan^{-1} \frac{\dot{y}}{\dot{x}}$
$\beta$	angle between relative velocity $\Delta V$ and the $x, y$ plane, $\tan^{-1} \frac{\dot{z}}{\sqrt{\dot{x}^2 + \dot{y}^2}}$
$\gamma$	flight-path angle between local horizon and $V$ , positive upward
$\epsilon$	eccentricity of space station orbit
$\zeta$	separation angle between ferry and orbital plane of station as measured from center of earth, positive when station is on right side of ferry
$\eta_f$	angle between orbital plane of space station and velocity component $V_t$
$\Theta$	angular position of space station as measured in plane of its orbit about center of earth. (In an elliptic orbit, $\Theta = 0$ at perigee; in a circular orbit, $\Theta = 0$ at rendezvous.)
$\Theta_f$	angular position of ferry, measured in plane of station's orbit from position $\Theta = 0$
$\Delta \Theta$	separation angle between ferry and station as measured in plane of station orbit from center of earth, positive when station is ahead of ferry

$\tau$	a specific value of time
$\Omega$	total angular velocity of space station
$\omega$	constant chosen to be exactly equal to $\dot{\theta}$ when space station is in exactly a circular orbit

## Subscripts:

$a$	apogee position
$c$	circular
$e$	earth
$f$	ferry vehicle
$o$	initial values at a specific position
$p$	perigee position
$s$	space station
$L$	launch values where launch occurs at end of boost period
$max$	maximum

Derivatives with respect to time are denoted with dots over the variables. For example,  $\frac{d\theta}{dt} = \dot{\theta}$ .

Vectors are denoted by bold face letters.

## ANALYSIS

## MISSION CONCEPT

The rendezvous mission is herein separated into two major phases: the rendezvous with another vehicle in an established orbit, and the return from that orbit back to earth. If the problem is restricted to a coasting phase outside of the sensible atmosphere of the earth, both problems can be studied simultaneously by investigating the trajectories in both positive and negative time. This approach will be the one used in this analysis.

The study is based on the assumption that the space station is in an arbitrary orbit and that the boost vehicle for the ferry is sufficiently powerful to launch the ferry into a variety of coasting trajectories, one of which is exactly right for the rendezvous based on the position of the station at the time of launch (booster burnout). The family of trajectories to be considered is illustrated in figure 1. As one deviates from a Hohmann ellipse (shown on the left-hand side of fig. 1), there is a family of transfer trajectories with apogee greater than the orbital altitude of the station or with perigee within the sensible atmosphere. On such trajectories rendezvous is to be achieved either during the ascending or during the descending phase of the transfer trajectory.

The problem investigated is essentially that of

determining the range of conditions over which a ferry can be launched and can still follow a trajectory which terminates at the space station. Rather than launch the ferry over a range of conditions and eliminate those trajectories that do not lead to rendezvous, the problem is treated in reverse. All calculations start with the ferry adjacent to the station at time zero. The ferry is given an incremental velocity component relative to the station and the equations of motion are solved in negative time for the rendezvous phase and in positive time for the return phase. (It will be shown in a subsequent section that with the proper interpretation, both results can be obtained by considering only one problem—either rendezvous or return.) In all cases the velocity and position of the ferry are calculated until the ferry vehicle reaches some reference altitude above the earth, taken to be 60 statute miles or until a minimum altitude is reached. The conditions at the 60-mile altitude are considered launch conditions for the rendezvous mission or entry conditions for the return mission.

The term launch is used to refer to the end of the boost phase and the start of the coasting phase on the ascent trajectory. Although current boost vehicles cannot, in general, achieve near-orbital velocities at 60 miles, future boost vehicles approach this condition. Reference 5 describes the desirability of achieving booster burnout at an altitude (above the atmosphere) as low as possible and coasting up to orbital altitude where a small additional velocity is applied for injection into orbit.

In this study it is not required that the relative velocity between the two vehicles be zero at the time of rendezvous since it is assumed that thrust control will be employed during the terminal phase to insure that the relative velocity and displacement are brought to zero simultaneously. However, in establishing the ground rules for this study, it is considered that this velocity correction should be of reasonable magnitude and should require a discharge of mass that would not exceed 10 or 15 percent of the mass of the launched ferry vehicle.<sup>1</sup>

It is further assumed that the trajectories of the two bodies (the station and ferry vehicle) do not

<sup>1</sup> A transfer ellipse having a perigee at 60 miles and an apogee at 300 miles above the earth will require a 366 feet per second increase in velocity for injection into a 300-mile circular orbit. With  $I_{sp}$  of 250 seconds, this value represents a minimum reduction in mass of about 4.0 percent.

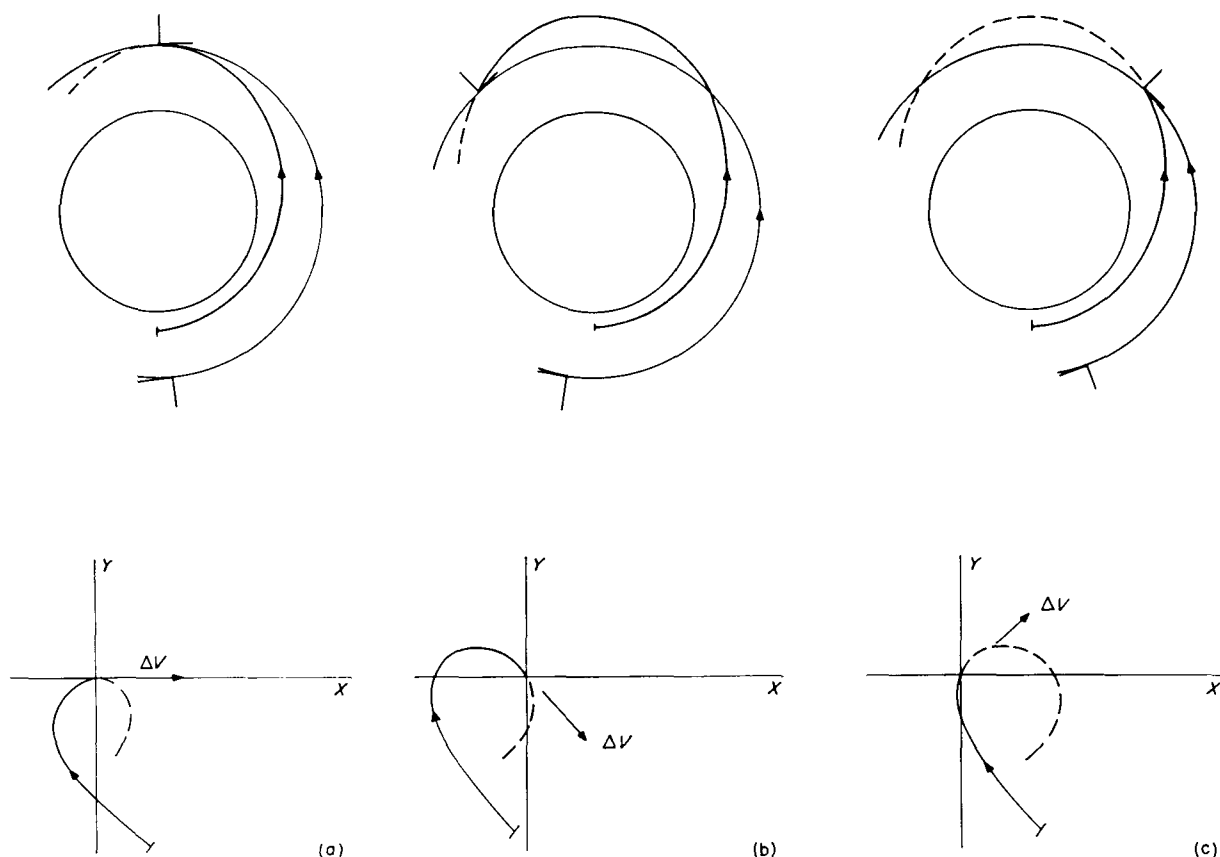


FIGURE 1.—Three typical trajectories of a ferry during a rendezvous with an orbiting space station. Upper figures show the trajectories as seen by an inertial observer; lower figures show the trajectories as seen by an observer in the space station. Station coordinates are  $X$  and  $Y$ ;  $\Delta V$  is the relative velocity of the ferry with respect to the station at the time of rendezvous.

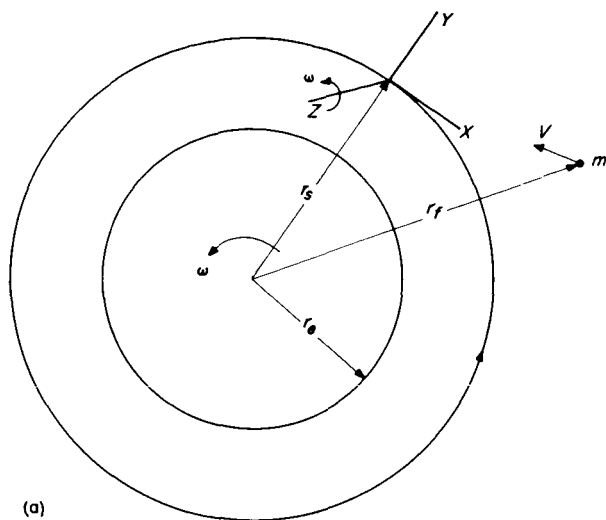
have to be in the same plane at the time of launch but their planes should intersect prior to or at the point of interception. The alternative (where the ferry is injected into an intersecting orbit) would make the injection guidance more difficult and the out-of-plane correction after injection more expensive. Therefore, in this study the relative velocity vector of the ferry vehicle at interception does not necessarily lie in the plane of the station's orbit. The implication in these last two assumptions is that terminal and probably midcourse guidance will be available to produce minor modifications to the nominal coasting trajectories obtained herein.

#### EQUATIONS OF MOTION

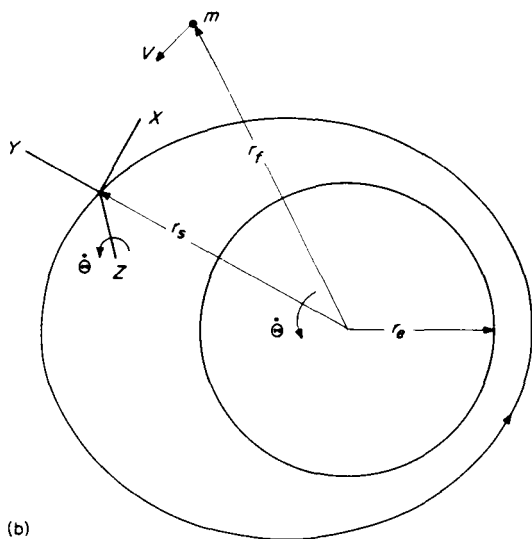
The equations of motion employed describe the motions of a mass, the ferry, moving in a radially symmetric gravitational field whose center is the center of the earth. The motions of the mass are

measured in a rotating set of coordinates whose origin is located at the center of the space station. The space station moves about the center of the gravitational field in a Keplerian trajectory at an angular velocity of  $\Theta$  which is a constant  $\omega$  only if the trajectory is a circle. The coordinate system moving with the station is composed of a rectilinear set of axes with the  $Z$ -axis normal to the orbital plane. The  $X$ - and  $Y$ -axes are rotated about the  $Z$ -axis at the same angular velocity  $\Theta$  so that the  $Y$ -axis always points away from the center of the earth. A schematic drawing of the coordinates of the problem are shown for the station in a circular orbit (fig. 2(a)) and in an elliptic orbit (fig. 2(b)).

The equations of motion of a mass with respect to a coordinate system fixed in a space station moving in a noncircular orbit (the more general case) are derived in appendix A. The variations of the station coordinates  $r_s$  and  $\Theta$  are then



(a)



(b)

(a) Station in circular orbit.

(b) Station in elliptic orbit.

FIGURE 2.—Coordinates employed in describing the motions of mass  $m$  in the space-station coordinate system.

described by the Keplerian equations of motion for which the solutions are well-known. For the special case where the space station is in a circular orbit and  $r_s$  and  $\dot{\theta}$  are constants, the equations of motion reduce to a form given in appendix B. Also given in appendix B are some approximate solutions to these equations which may be used when the distance from the mass to the origin of the coordinate system is small compared with  $r_f$ . These approximate solutions were reported in references 6 and 7. Since neither reference 6 nor reference 7 gives the derivation, it

has been included in appendixes A and B.

The inertial position and velocity of the ferry is also important for various purposes such as the calculation of launch conditions. Transformations for the position and velocity data from the rotating orbiting frame of axes to the nonrotating earth-fixed axes are given in appendix C.

## DESCRIPTION OF MOTION

Since the motion of a body with respect to a rotating coordinate system moving in a central gravity field has certain unique characteristics, some description of that motion is given. Consider at time zero a mass located at the center of the rotating coordinate system where the system is moving in a circular orbit. If that mass has an initial relative velocity  $\Delta V$  in the plane of the orbit, the mass will at subsequent times move out from the origin on a curved path. This condition is illustrated in figure 3 for the case of the coordinate system moving counter-clockwise in a circular orbit of radius  $r_s = 4,260$

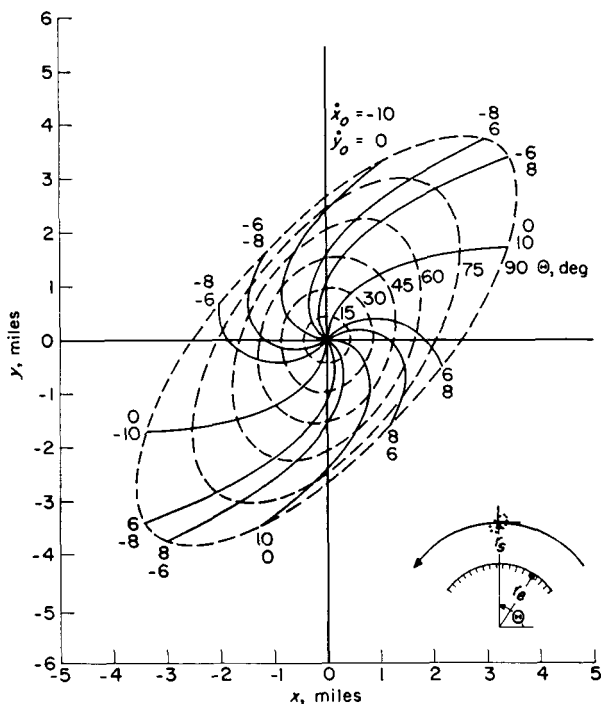


FIGURE 3.—Trajectories of a number of point masses ejected from the center of the rotating coordinate system at  $t=0$  ( $\theta=0$ ), each with a total relative velocity of 10 feet per second, but with different velocity components. The solid lines are discrete trajectories; the dashed lines are the contours of the positions of the masses at subsequent positions of the coordinate system.

miles out from the center of the earth ( $h_s=300$  miles). In figure 3 trajectories are shown for the mass with several different combinations of initial velocity components. In each case the total relative velocity is 10 feet per second. The angular velocity of the coordinate system  $\omega$  is constant so that the subsequent position of the mass is defined at any time  $t$  when the coordinate system has moved  $\omega t = \theta^\circ$  around the earth. Dotted lines have been used to join the positions at certain values of  $\theta$  up to  $\theta=90^\circ$ . It can be seen that, if a mass has a relative velocity radially outward from the earth (along the  $Y$ -axis so that  $\dot{x}_0=0$ ,  $\dot{y}_0=10$ ), then, as its radial distance from the center of the earth becomes larger, the angular velocity of the mass becomes less than that of the coordinate system, and the mass moves up and behind the coordinate system. Likewise a mass having a relative velocity along the positive  $X$ -axis ( $\dot{x}_0=10$ ,  $\dot{y}_0=0$ ) will initially have a lower angular velocity than the coordinate system and will move back and below the coordinate system. As the mass moves closer to the earth, the angular velocity increases and the mass moves ahead of the coordinate system. For other combinations of  $\dot{x}$  and  $\dot{y}$  the mass will follow similar trajectories. The locus of points on these trajectories at equal values of time (or  $\theta$ ), shown by the dashed lines in figure 3, is first a circular pattern and later an elliptical pattern about the coordinate center.

It would appear that the trajectories of figure 3 are antisymmetric. For small relative velocities and values of  $\theta=\omega t$ , this is approximately true. However, the spherically symmetric gravity field changes this condition; thus, the motions are actually antisymmetric about a curvilinear coordinate system defined by the  $Y$ -axis and the line of constant  $r_s\theta$  as shown in figure 4.

The effect of this spherical gravity field on the motions of a mass is shown in figure 5 for two special cases. In figure 5(a) the mass has an initial velocity of 400 feet per second directed along the  $Y$ -axis of the coordinate system. In figure 5(b) the mass has the same velocity but the velocity is directed along the positive  $X$ -axis of the coordinate system. Shown on the left-hand side of figure 5 are the relative motions of the mass and the coordinate system as seen by an inertial observer. On the right-hand side the same trajectory is shown as viewed by an observer in the center of the coordinate system. In order to

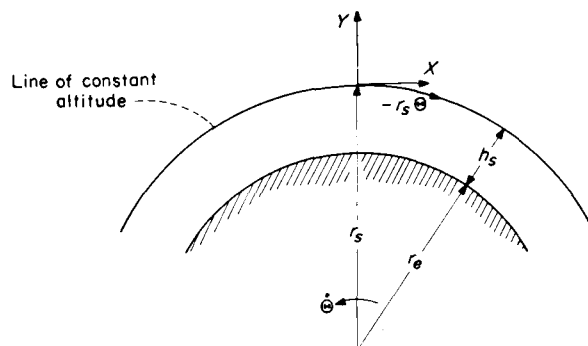


FIGURE 4.—Rectilinear and curvilinear coordinates. 1

simplify the definition of the direction that  $\Delta V$  makes with the coordinate system, the angles  $\alpha$  and  $\beta$  are introduced and are defined as

$$\alpha = \tan^{-1} \frac{\dot{y}}{\dot{x}}$$

$$\beta = \tan^{-1} \frac{\dot{z}}{\sqrt{\dot{x}^2 + \dot{y}^2}}$$

Thus,  $\beta$  is the angle that  $\Delta V$  makes with the  $x, y$  plane of the coordinate system and  $\alpha$  is the angle that the in-plane component of  $\Delta V$  makes with the  $x$ -axis. If  $\Delta V$  lies entirely in the plane of the orbit of the coordinate system ( $z=\dot{z}=0$ ), then  $\alpha$  is simply the angle that  $\Delta V$  makes with the  $x$ -axis.

In figure 5(a), the value of  $\alpha$  is  $90^\circ$  and the trajectory starts at  $\theta=0^\circ$ . The trajectory of the mass is an ellipse with apogee at  $\theta=90^\circ$  and perigee at  $\theta=270^\circ$ . When  $\theta$  is  $360^\circ$ , the mass has returned again to the center of the coordinate system. In this special case, the mass had the same orbital period as the coordinate system. This condition is the result of assuming a spherical gravity field. If the oblateness of the earth were taken into account, the orbital periods would not be the same. In a spherical gravity field this condition is always true for any relative velocity of the mass, when the angle  $\alpha$  is equal to  $90^\circ$  or  $270^\circ$ .

Figure 5(b) shows the case where  $\alpha=0^\circ$ . The trajectory starts with  $\theta=0^\circ$  and the inertial velocity of the mass 400 feet per second less than that of the coordinate system. Because of this smaller inertial velocity, the centrifugal force of the mass is less than that of the coordinate system and the mass initially falls behind and below. The period of the mass is shorter than that of the



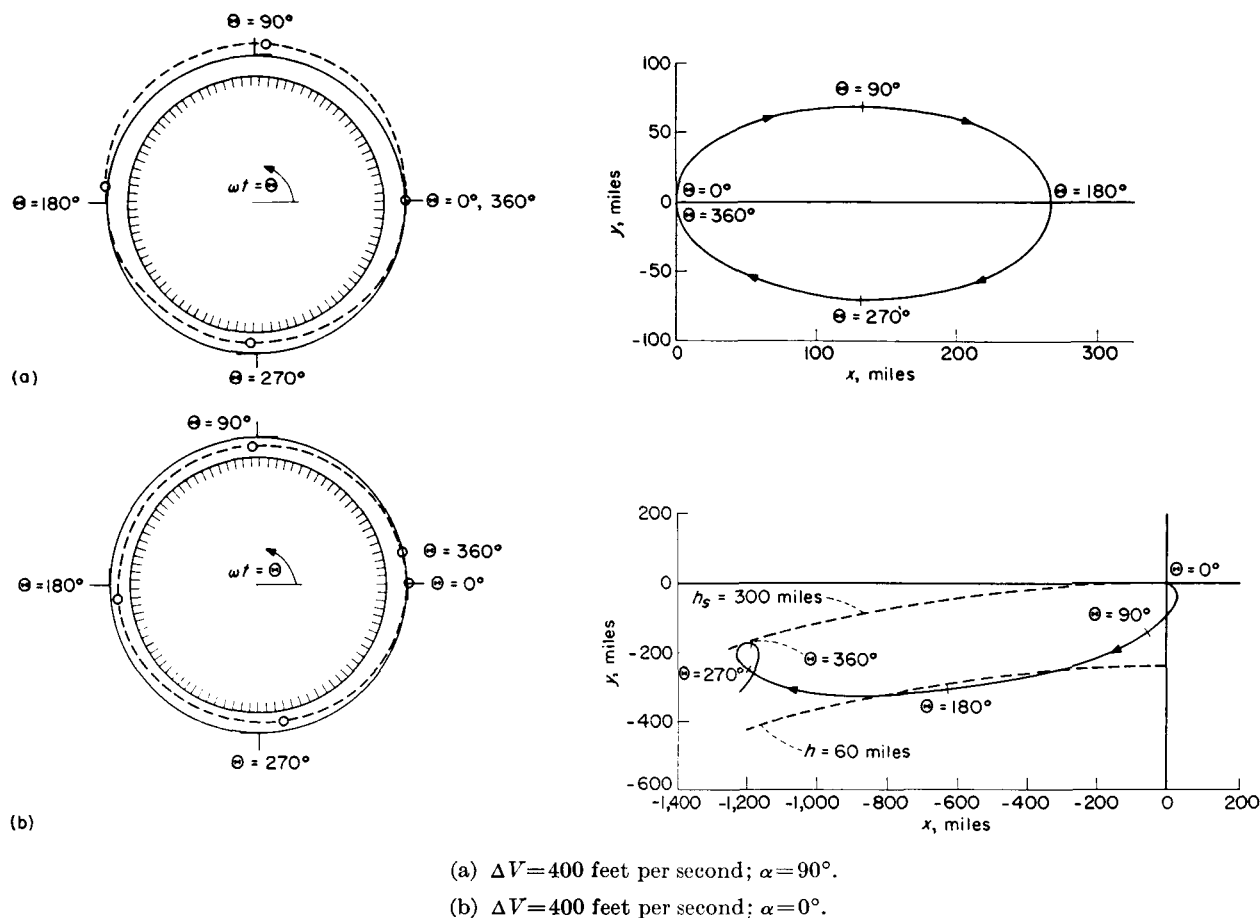


FIGURE 5.—Two typical trajectories of a mass which at  $t=0$  ( $\theta=0$ ) was at the center of the coordinate system and had a relative velocity  $\Delta V$ , which made an angle  $\alpha$  with the  $X$ -axis. Trajectories are shown as viewed by an inertial observer (on the left) and an observer in the center of the coordinate system (on the right).

coordinate system in this case; therefore, after the coordinate system has made one complete revolution about the earth, the mass is roughly 1,200 miles ahead of the  $Y$ -axis and 180 miles below the  $X$ -axis. Because of the curvature of the earth, however, both the mass and the coordinate system are at approximately the same altitude of 300 miles. The curvilinear coordinate  $r_s\theta$  is shown in figure 5(b) as the line of constant  $h_s$ , which is, in this case, 300 miles above the mean earth.

#### COMPARISON OF MOTIONS OBTAINED FROM EXACT AND APPROXIMATE EQUATIONS

Since the equations of motion of a mass in terms of the rotating coordinate system are amenable to approximate solutions, it may be desirable at this point to examine the motions as computed from the approximate equations and to consider whether

motions so calculated are satisfactory for use in the problem under consideration.

In appendix B, approximate solutions are obtained for the case where the coordinate system is in a circular orbit. The approximate equations were obtained by expanding the gravity term into a Taylor series (in powers of  $x$ ,  $y$ , and  $z$ ) and dropping all terms higher than the first order. The effect of this approximation on the calculated motions of the mass is illustrated in figure 6. At  $t=0$  the mass was at the center of the coordinate system and had a relative velocity of 200 feet per second in the direction  $\alpha=45^\circ$ . Subsequent trajectories were computed in both positive and negative time by using both the approximate and the exact equations of appendix B. In the upper half of figure 6 is shown the variation of  $y$  with  $x$  of the trajectory in terms of the rotating coordinate system. Shown in the lower half of figure 6

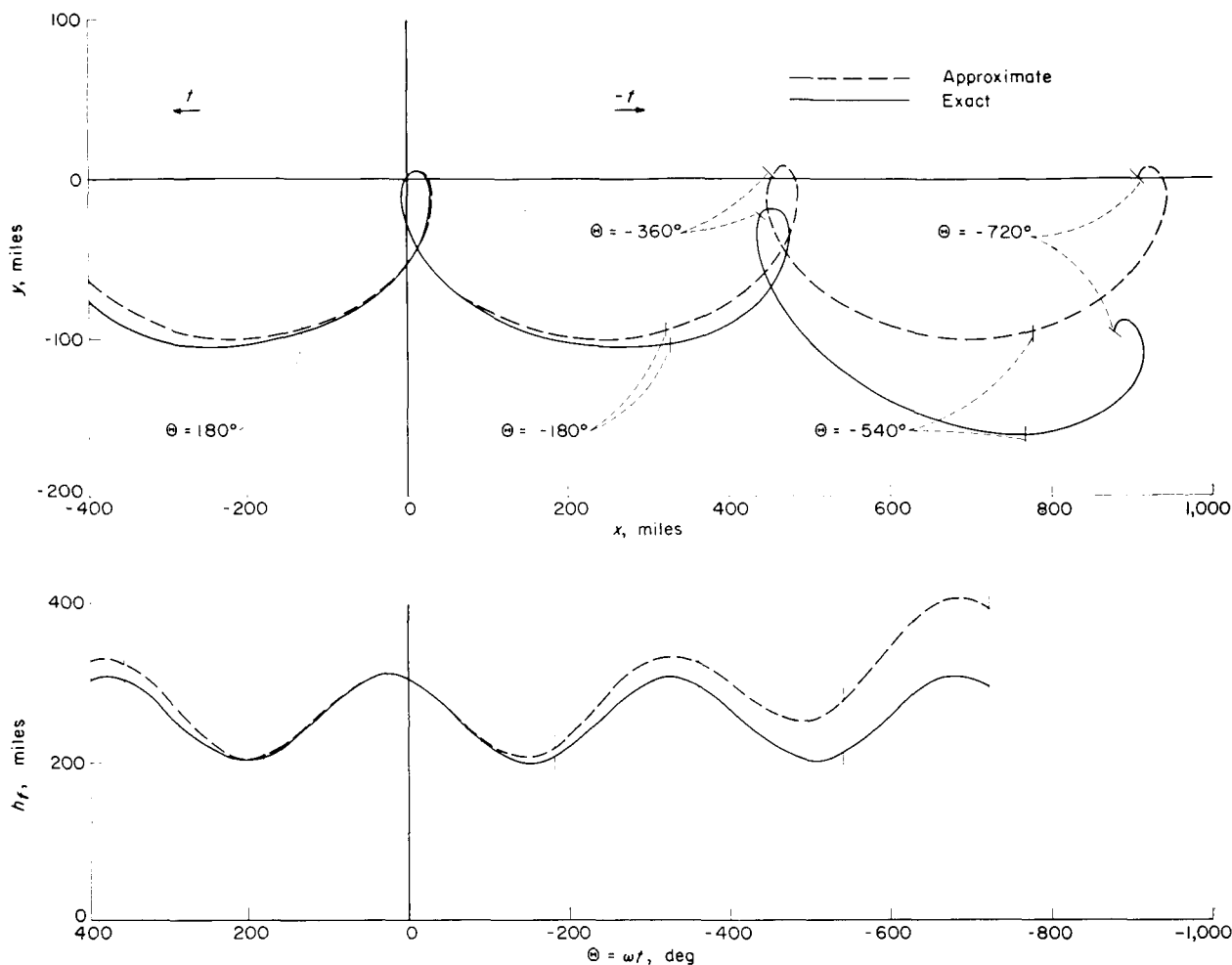


FIGURE 6.—Comparison of two trajectories obtained by solving exact and approximate equations of motion in both positive and negative time. At  $t=0$  both the approximate and the exact equations had the same initial conditions:  $\Delta V=200$  feet per second,  $\alpha=45^\circ$ ,  $\beta=0^\circ$ .

s the variation of the altitude of the mass designated as  $h_f$ , the distance above the mean surface of the earth. It may be seen that, for values of  $|\theta| \leq 90^\circ$ , the differences between the approximate and exact solutions are fairly small. By the time the coordinate system has made one complete revolution about the earth, it may be seen that the differences between the two solutions become very large. Within the first order of magnitude, this error is directly a function of  $\theta$  and not of  $x$  or  $y$ . The trajectory of the mass as computed by the approximate equations appears to be the result of a gravity field parallel to the  $Y$ -axis. The approximation that the gravity field is parallel while the earth and actual gravitational field are

curved results in an apparent increase in  $h_f$  with each orbital revolution. With these approximate equations, errors in velocity and acceleration are obtained similar to those obtained in the position of the mass.

From this cursory examination, it would appear that motions obtained from the approximate equations are usually adequate when the mass is in close proximity to the coordinate system and  $\theta$  is less than, for example,  $90^\circ$ . However, for the case under consideration  $\theta$  and the separation distance may become relatively large, and it would appear that motions computed from the approximate equations would not be sufficiently accurate. Therefore, only the exact equations are used in the subsequent sections of this paper.

## SOLUTIONS OBTAINED IN POSITIVE AND NEGATIVE TIME

In order to obtain a rendezvous between a space station already in orbit and a ferry vehicle which is launched from the earth, the ferry vehicle must be put onto a trajectory which intersects or nearly intersects the orbital track of the space station. Likewise, when the ferry leaves the space station for the return trip to some desired landing site on earth, it must be put onto a trajectory which intersects the earth's atmosphere at some predetermined position. Both trajectories may be computed by placing the mass, which in this case is the ferry, at the center of the station's coordinate system and running the problem in negative or positive time. Figure 7 illustrates two such trajectories calculated in both positive and negative time.

One trajectory, shown in figure 7 with a solid line, represents the trajectory of the ferry vehicle

for the case where  $\Delta V$  was 200 feet per second and  $\alpha$  was  $-135^\circ$  at  $t=0$ . It may be seen that for both positive and negative time the trajectory of the ferry was at a greater orbital altitude than that of the space station. Ticks have been placed on the trajectory for every integral multiple of  $\theta$  of  $90^\circ$ , that is, every quarter revolution of the station about the earth. Although not shown, a trajectory obtained for  $\alpha=135^\circ$  also showed the same characteristic of moving away from the earth in either positive or negative time.

The trajectory shown with the dashed lines in figure 7 is a case where again  $\Delta V=200$  feet per second but  $\alpha=45^\circ$  at  $t=0$ . In this case the ferry reached a perigee altitude of 200 miles above the surface of the earth. This same perigee altitude was obtained for trajectories calculated in both negative and positive time and for  $\alpha=-45^\circ$  as well as for  $\alpha=45^\circ$ . Although this

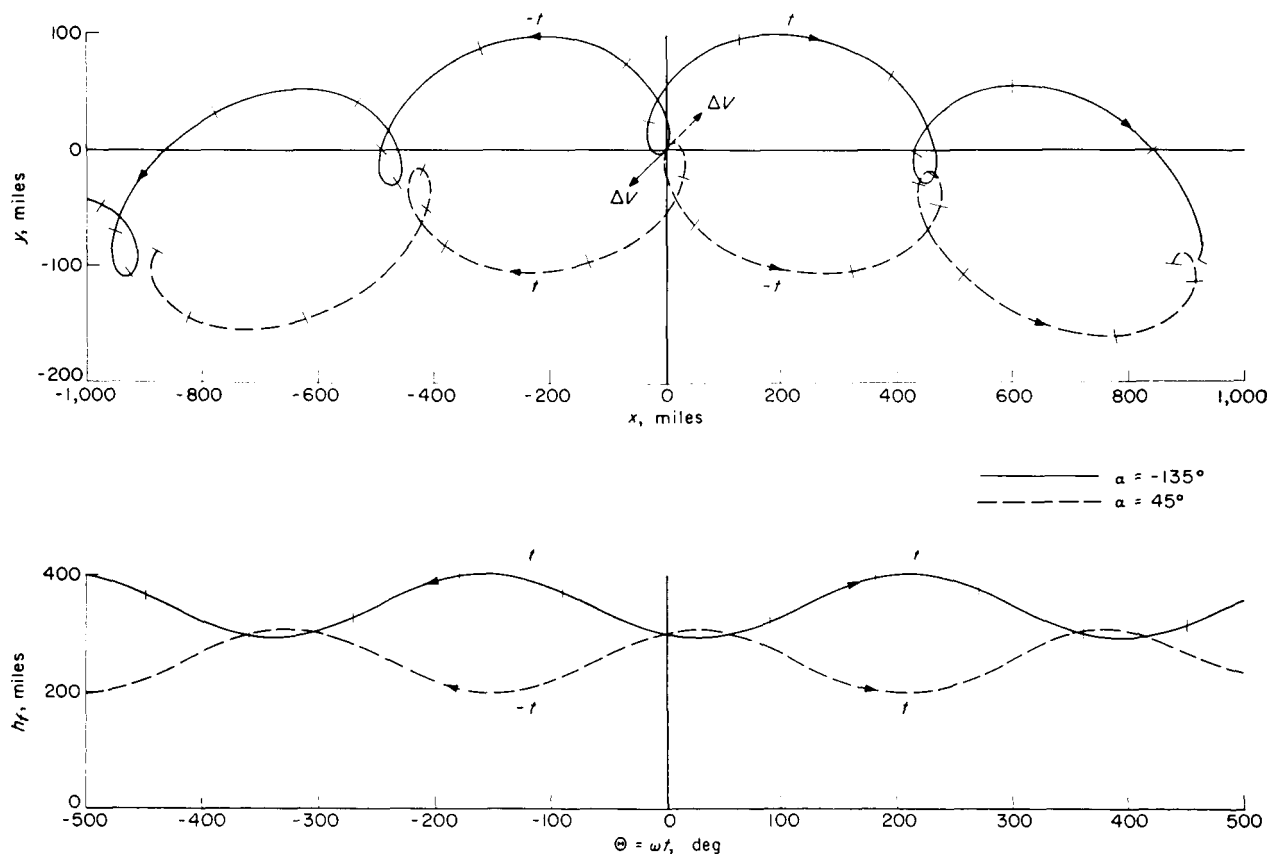


FIGURE 7.—Variation of two ferry vehicle trajectories computed in positive and negative time. Trajectories are shown in terms of the rotating coordinate system  $(x, y)$  of a space station in a circular orbit and in terms of altitude measured from the surface of the earth. At  $t=0$  the ferry is at the center of the station coordinate system and has a relative velocity of 200 feet per second which makes an angle  $\alpha$  with the  $X$ -axis. Ticks are shown at every integral multiple of  $\theta=90^\circ$ .

altitude is still above that usually used to define the upper limit of the earth's atmosphere, the important point is that, when  $|\alpha|$  was  $45^\circ$ , the ferry moved toward the earth, and, when  $|\alpha|$  was  $135^\circ$ , the ferry moved away from the earth.

A general rule may be stated here for the case of a station in a circular orbit: For either rendezvous or return trajectories and for a given relative velocity  $\Delta V$  at the time of intersection of the station and ferry, the trajectory leading to the smallest perigee will have a relative velocity  $\Delta V$  which makes an angle  $\alpha=0^\circ$  with respect to the  $X$ -axis (that is, the case where the trajectory of the ferry is a Hohmann ellipse). As  $|\alpha|$  increases, the perigee altitude will increase until at  $|\alpha|=180^\circ$  the perigee altitude of the ferry is equal to the orbital altitude of the station. Thus, if the ferry is to go from the station to the proximity of the earth, or vice versa, with a near-minimum amount of energy, the relative velocity at the time of intersection will be in the first or fourth quadrants ( $-90^\circ < \alpha < 90^\circ$ ). If  $\Delta V$  is large enough and lies in the second or third quadrants, close proximity to the earth can be achieved but the inertial velocity will always be larger than if  $\Delta V$  were in the first or fourth quadrants.

In the case of  $\alpha=-135^\circ$  in figure 7, it may be seen that the trajectory had a perigee only a few miles closer to the earth than the altitude of the station. In the case of  $\alpha=45^\circ$ , perigee was 100 miles closer to the earth. The same would be true for  $\alpha=135^\circ$  and  $\alpha=-45^\circ$ . Therefore, most of the trajectories studied in the remainder of this paper will be those where  $\alpha$  lies in the first or fourth quadrants ( $|\alpha| \leq 90^\circ$ ).

### RESULTS

By using the equations derived in appendixes A, B, and C, numerical results have been obtained for two particular orbits of a space station. In the first case, the station was assumed to be in a circular orbit 300 miles above the earth. In the second case, the station was assumed to be in an elliptic orbit having a perigee of 100 miles and an apogee of 500 miles so that the nominal orbital altitude was 300 miles. Only results for the rendezvous mission are shown and discussed. However, the associated case of the return trajectory of the ferry from the station to the earth (obtained by solving the equations of motion in

positive time) are symmetric reflections (about the  $Y$ -axis) of the rendezvous trajectories. Thus the rendezvous trajectories to be shown can also be interpreted as return trajectories by simply reversing the direction of  $\Delta V$  and the direction of the station rotation. This interpretation is illustrated in figure 8. With this interpretation the launch conditions discussed for the rendezvous mission

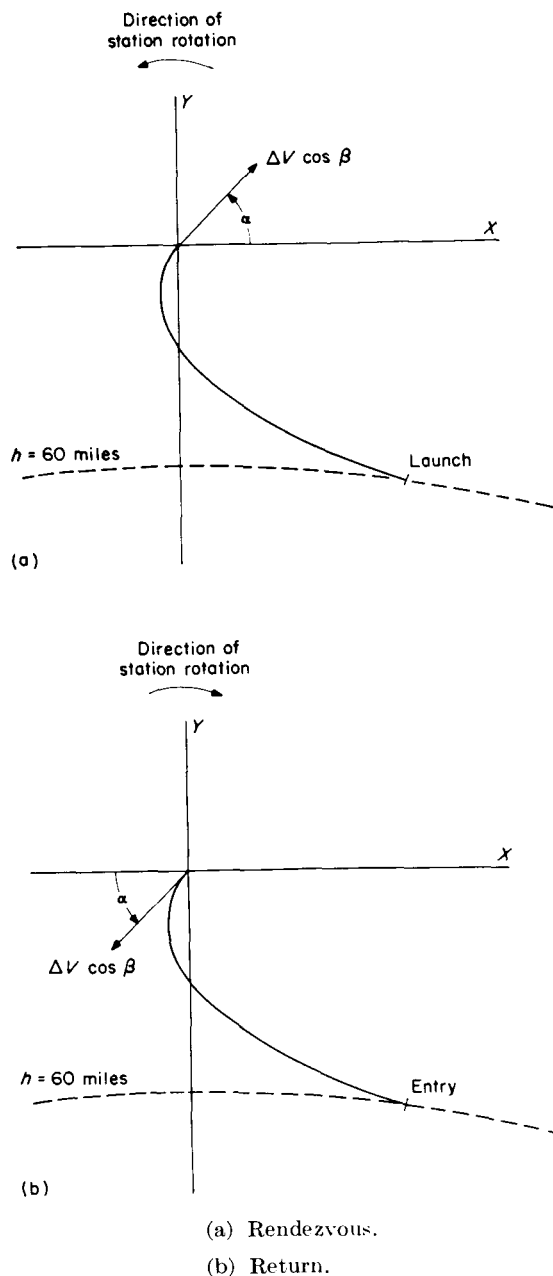


FIGURE 8.—Rendezvous and return trajectories.

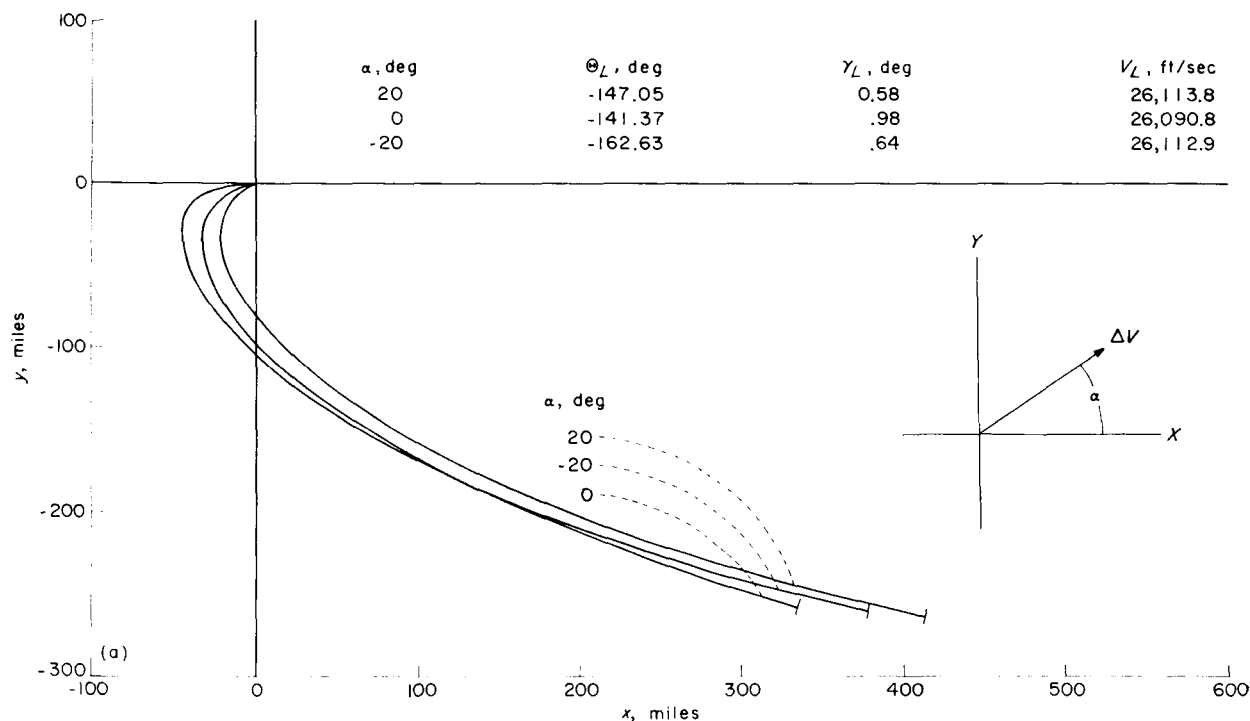
can be also treated as the entry conditions for the return mission.

#### STATION IN A CIRCULAR ORBIT

The trajectories leading to rendezvous of a ferry with the space station in a 300-mile circular orbit were obtained by placing the ferry at the center of the station's coordinate system at  $t=0$  and solving the equations of motion in negative time. Five cases of relative velocity  $\Delta V$  were studied: 200, 400, 600, 800, and 1,000 feet per second. The angle  $\alpha$  was varied from  $-90^\circ$  to  $90^\circ$ . The results of these trajectories are shown in figures 9 to 13.

**Coplanar trajectories.**—The first trajectories presented are those obtained for the case where the entire motion of the ferry vehicle takes place in the plane of the station's orbit. Shown in figure 9 are a number of typical trajectories where the motion is described in terms of the  $x, y$  coordinate system of the station. It was assumed in these trajectory calculations that booster burnout occurred just above the sensible atmosphere of the

earth, an altitude which was chosen to be 60 miles. Those trajectories which intersect the 60-mile altitude were considered to be possible rendezvous trajectories. Ticks are placed on the trajectories at this point. The results for the case of  $\Delta V=200$  feet per second are not shown since none of the trajectories constitute possible rendezvous trajectories from a booster burnout altitude of 60 miles. From orbital mechanics calculations it may be shown that the minimum injection velocity (that is, closing velocity) is approximately 360 feet per second for the in-plane case considered. In figure 9(a),  $\Delta V=400$  feet per second and trajectories having an  $|\alpha| \leq 20^\circ$  are shown to be possible rendezvous trajectories. For  $|\alpha| \geq 30^\circ$ , rendezvous trajectories from an altitude of 60 miles were not possible. Figure 9(a) illustrates that at booster burnout the ferry can be anywhere from 335 to 415 miles behind the space station, a spread of 80 miles. Since the station is traveling at a rate of approximately 5 miles per second over the surface of the earth, this distance represents a spread in



(a)  $\Delta V=400$  feet per second.

FIGURE 9.—Variation of  $y$  with  $x$  for a series of trajectories of a ferry vehicle during rendezvous with a space station in a 300-mile circular orbit. The ferry intersects the space station with a velocity  $\Delta V$  and an angle of closure  $\alpha$ . All trajectories are in the orbital plane of the station. Ticks are used to denote those trajectories which start at a 60-mile altitude.

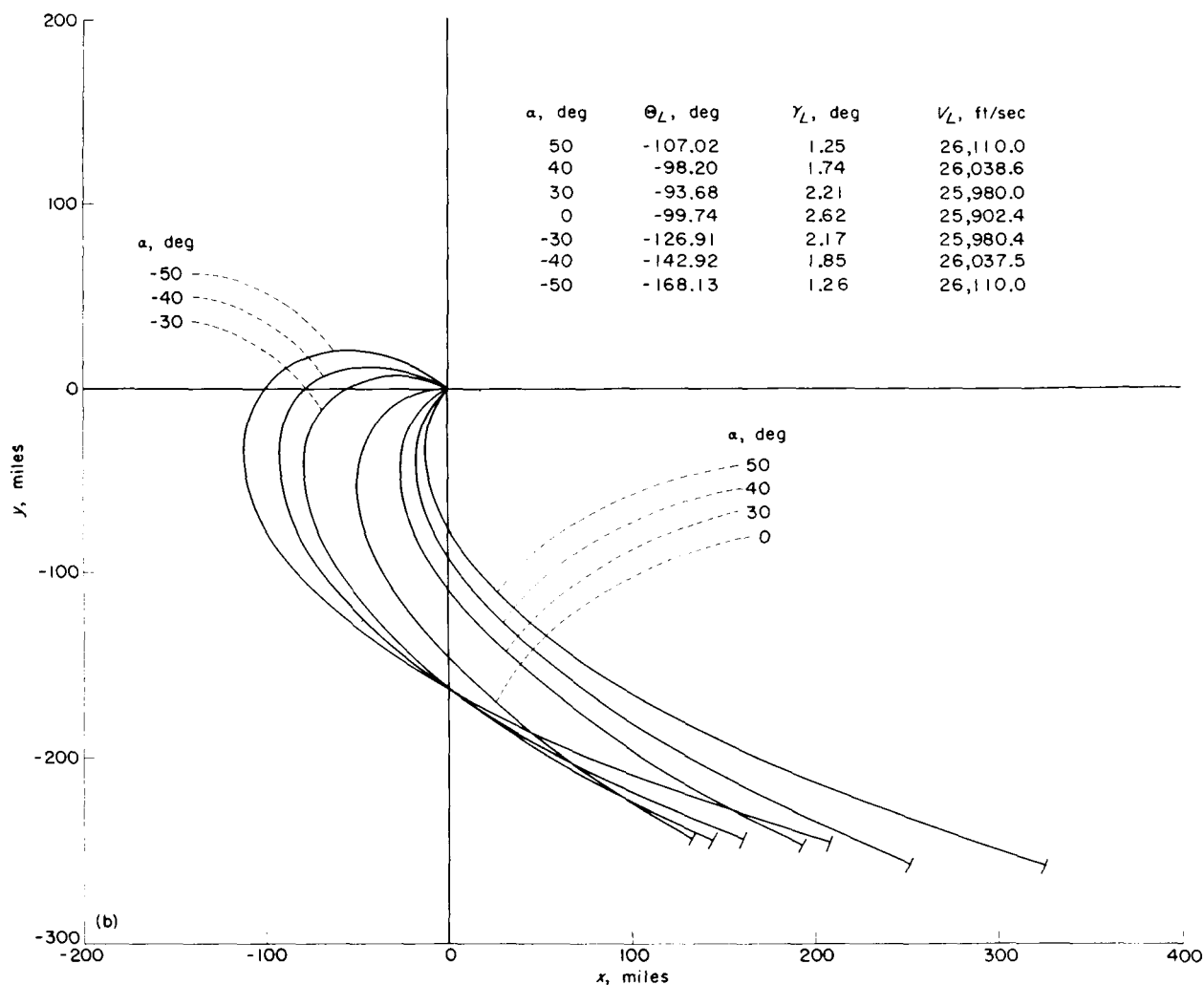
(b)  $\Delta V = 600$  feet per second.

FIGURE 9.—Continued.

launch time of 16 seconds. Thus, as the angle of closure  $\alpha$  opens up, so does the range of launch conditions and launch times. A similar analysis may be made from figures 9(b), 9(c), and 9(d) where  $\Delta V$  equals 600, 800, and 1,000 feet per second, respectively.

Also shown in these figures is a tabulation of the launch conditions for each of the possible rendezvous trajectories. For each of these trajectories is listed the inertial velocity and flight-path angle of the ferry at launch, and the positional angle of the station at the time of launch  $\Theta_L$ . By definition,  $\theta$  at rendezvous is equal to zero. Again referring to figure 9(a), it may be seen from the tabulated data that from the time of booster

burnout to the time of rendezvous the space station travels between  $147^\circ$  and  $162^\circ$  around the earth. These values of launch conditions were obtained by simultaneously computing the inertial velocities by the method described in appendix C and by interpolating between the numerical data points to obtain the values at approximately 60 miles.

The trajectories were initially obtained at increments of  $\alpha$  of  $30^\circ$ . In order to investigate the trajectories that lay between possible and not possible rendezvous trajectories, additional intermediate cases were also calculated in  $10^\circ$  increments. Thus, the pattern of values of  $\alpha$  investigated for any one case may be irregular.

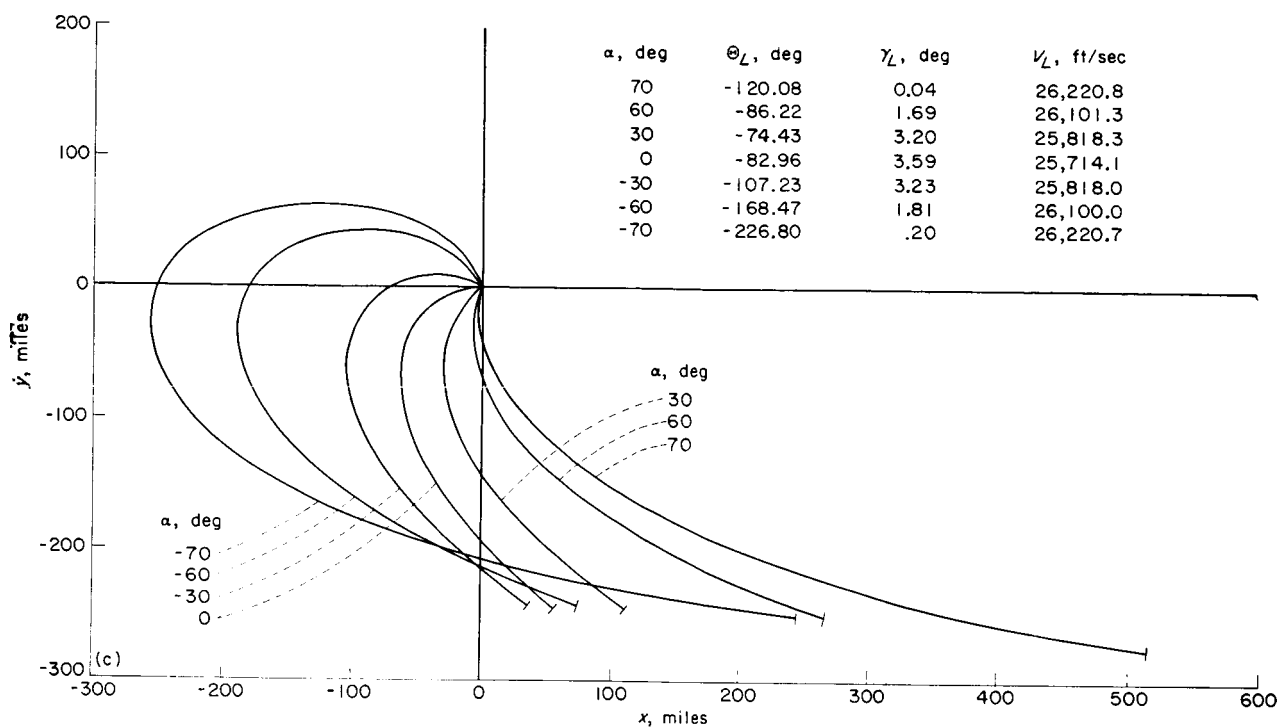
(c)  $\Delta V = 800$  feet per second.

FIGURE 9.—Continued.

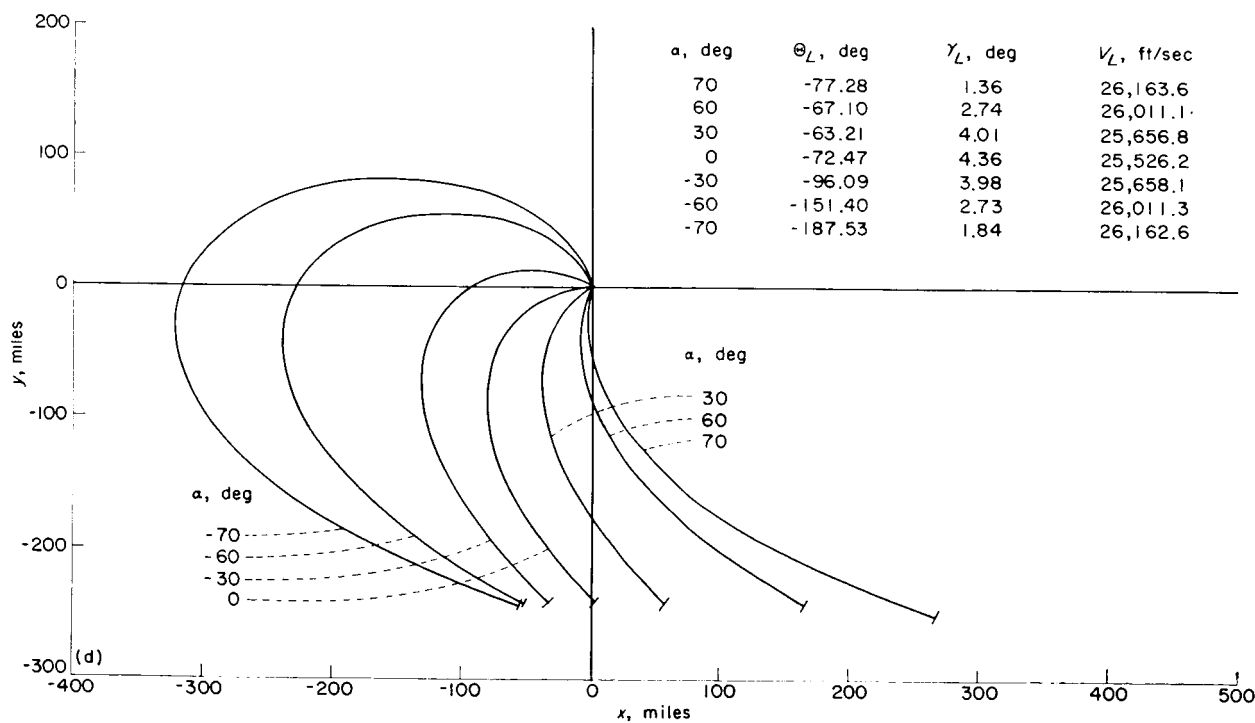
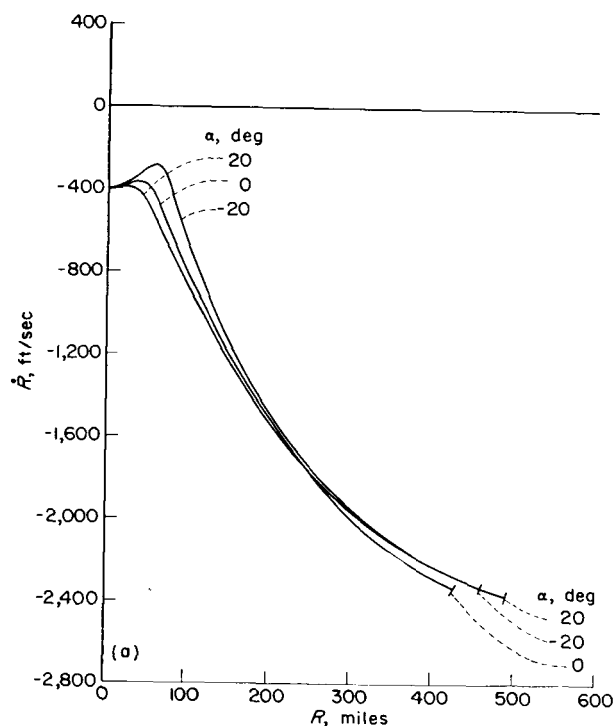
(d)  $\Delta V = 1,000$  feet per second.

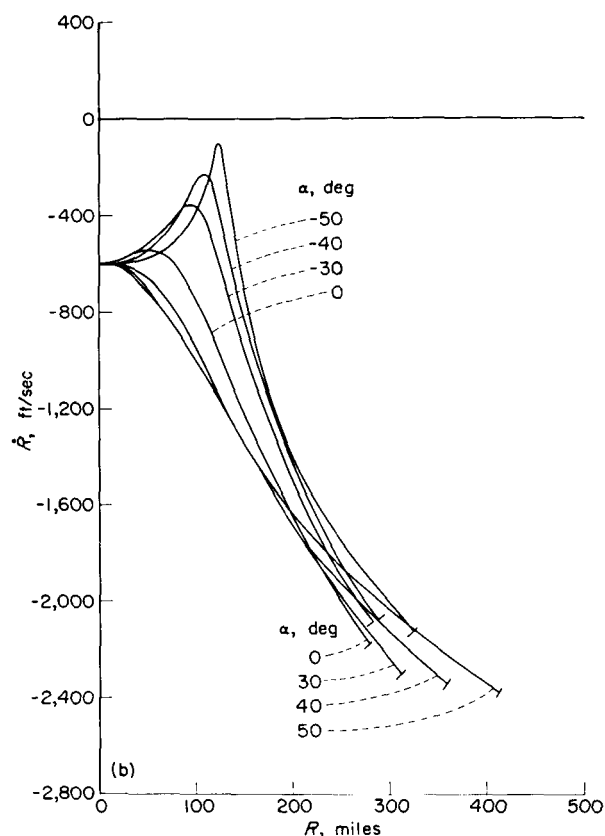
FIGURE 9.—Concluded.

In figure 10 the variation of range rate with range is shown for the same trajectories that were treated in figure 9. Ticks are again put on the end of each trajectory at the point where it intersected an altitude of 60 miles. It is of interest to note the wide variation of range rate with range between the trajectories which led to rendezvous. At closing velocities of 800 and 1,000 feet per second, one or more possible rendezvous trajectories achieved a positive value of range rate somewhere during the trajectory. This condition means that, for a while, the ferry vehicle was moving away from the space station. Such a phenomenon occurs when the ferry vehicle occupies a position ahead of and above the space station and rendezvous occurs on the descent from apogee. This condition leads to a large negative value for  $\alpha$ . (See cases illustrated in fig. 1(b).) If a display of range rate against range were the only information supplied to a human pilot during the midcourse phase of rendezvous, such a trajectory as this might lead to some consternation and doubt that rendezvous would indeed occur.



(a)  $\Delta V = 400$  feet per second.

FIGURE 10.—Variation of range rate with range for a ferry vehicle during rendezvous with a station in a 300-mile circular orbit. All trajectories are in the orbital plane of the station ( $\beta = 0$ ).



(b)  $\Delta V = 600$  feet per second.

FIGURE 10.—Continued.

In all cases it may be noted that range rate was essentially constant during the last few miles before rendezvous. This condition, which is synonymous with a collision course, is found to be of interest in the terminal phase of a rendezvous. Such a condition is illustrated in figure 10(e) for the case where the closing velocity was 600 feet per second. Shown in figure 10(e) is an enlargement of the last 60 miles for three of the trajectories shown in figure 10(b). It may be seen that during the last 60 miles the largest variation in range rate for any of the trajectories was 125 feet per second. In the last 12 miles (at a closing velocity of 600 feet per second, this value represents about 100 seconds of time) changes in range rate are virtually undetectable. Although the distance at which this condition occurred varied with the rate of closure, this trend is essentially the same whenever the ferry vehicle is on a collision course with the station.



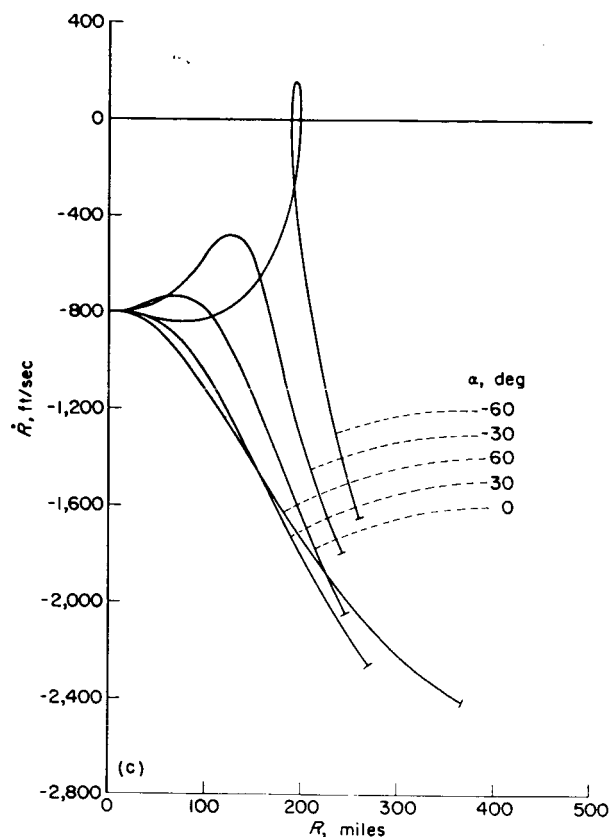
(c)  $\Delta V = 800$  feet per second.

FIGURE 10.—Continued.

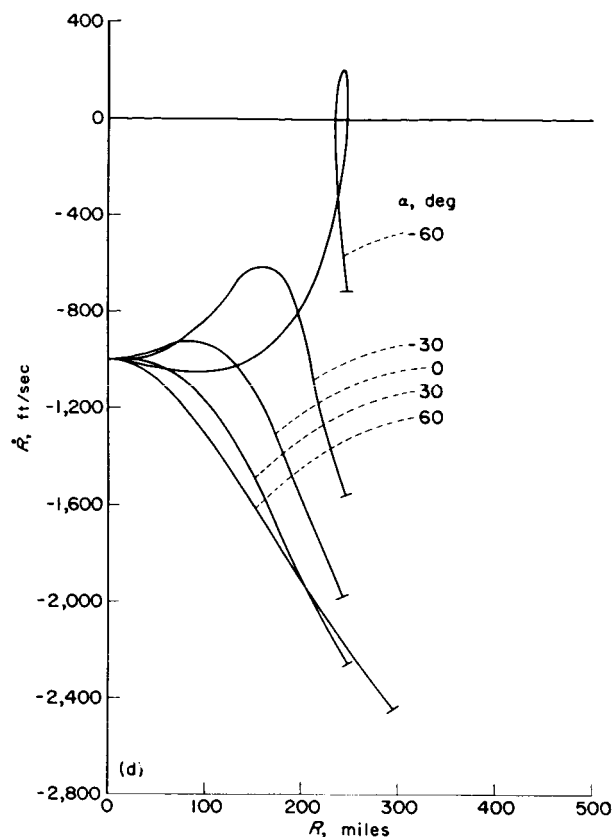
(d)  $\Delta V = 1,000$  feet per second.

FIGURE 10.—Continued.

**Out-of-plane trajectories.**—A number of the trajectories described in the previous section were also calculated with an initial out-of-plane velocity. For an in-plane velocity of 400 feet per second and a closing angle  $\alpha$  of  $0^\circ$  trajectories were obtained with values of  $\dot{z}$  at rendezvous of 200, 400, and 600 feet per second. These values of  $\dot{z}$  represent  $\beta$  angles of  $26.6^\circ$ ,  $45.0^\circ$ , and  $56.3^\circ$ , respectively. These three cases are shown in figure 11(a) in plots of  $y$  against  $x$  and  $y$  against  $z$ . It may be seen that each 200 feet per second of lateral velocity represents a maximum change in out-of-plane distance of about 34 miles. It may also be seen that the variation of  $y$  with  $x$  is virtually independent of any variation in  $z$ . The approximate equations of motion derived in appendix B resulted in solutions where  $z$  was independent of  $x$  and  $y$ . The results of figure 11(a) indicate that the approximation (that  $z$  is independent of  $x$  and  $y$ ) is fairly accurate, at least for half an orbital period. As a result of this condition, equation

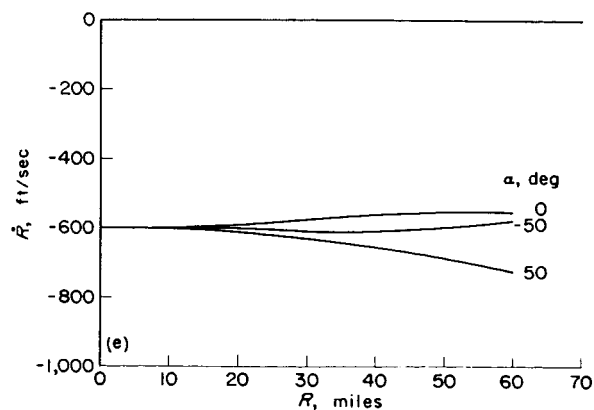
(e) Enlargement of three trajectories during the last 60 miles prior to rendezvous.  $\Delta V = 600$  feet per second;  $\beta = 0$ .

FIGURE 10.—Concluded.

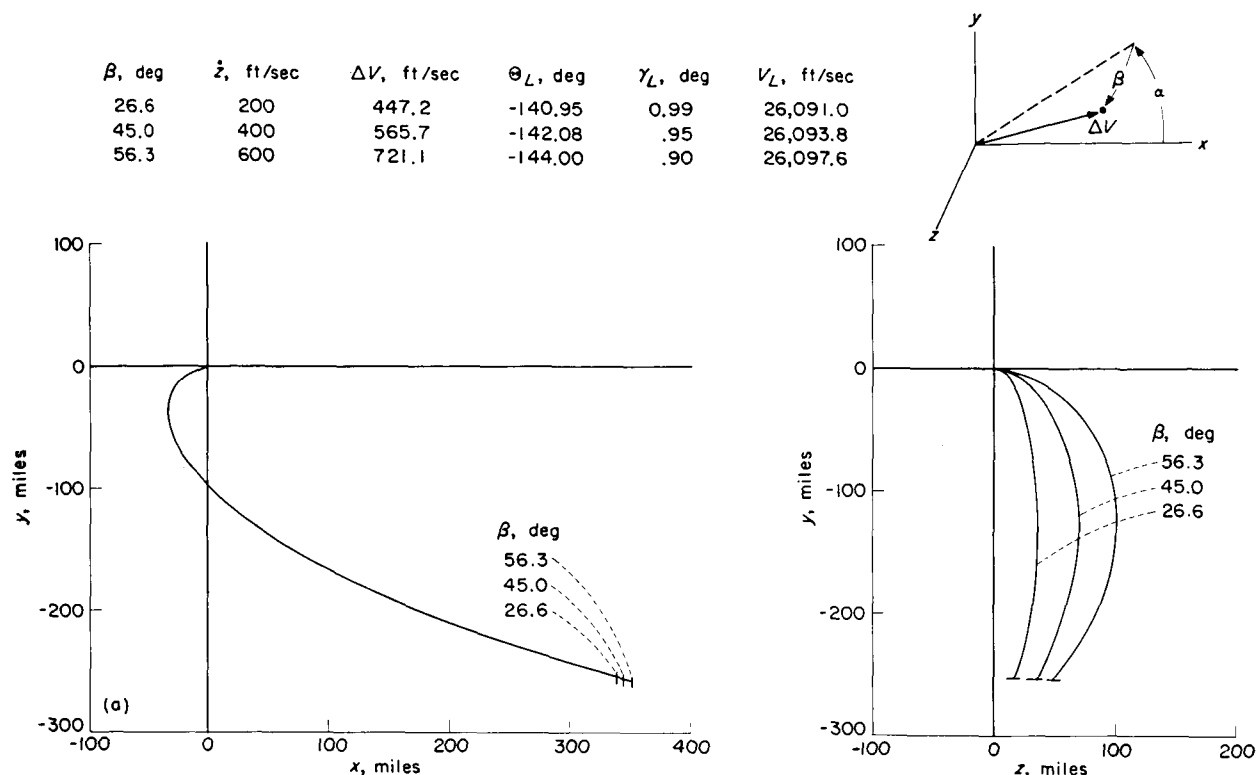


FIGURE 11.—Variation of out-of-plane trajectories in terms of  $x$  and  $y$  and  $z$  and  $y$  for the case of a ferry during rendezvous with a station in a 300-mile circular orbit.

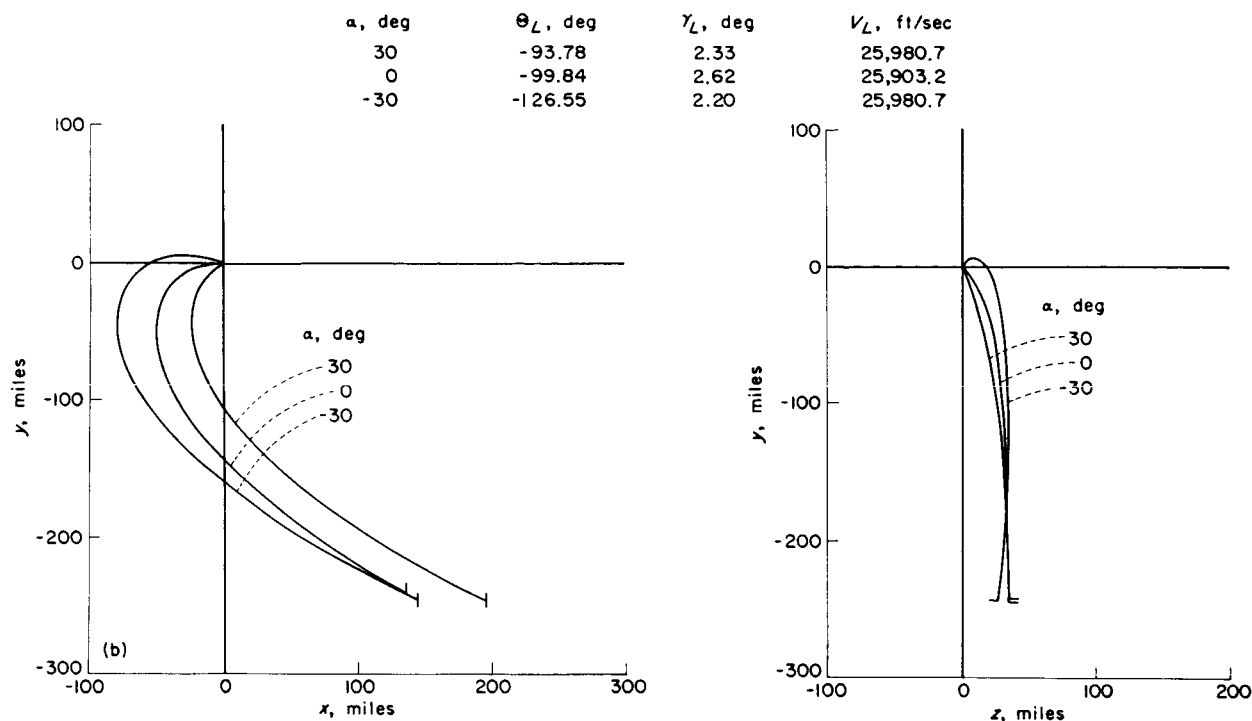
(B8) of appendix B may be used to compute a relationship for the maximum out-of-plane distance obtained. For a given orbital angular velocity of the station  $\omega$  and a given out-of-plane velocity  $\dot{z}_0$  evaluated at the time the ferry passes through the orbital plane, the maximum out-of-plane distance that can be obtained is

$$|z|_{\max} = \left| \frac{\dot{z}_0}{\omega} \right| \quad (1)$$

The physical analogy here is the simple harmonic motion of an undamped mass-spring system having a natural frequency of  $\omega$ . The motion takes place normal to the plane of the orbit and the total energy of this motion is conserved. Thus, the maximum kinetic energy ( $\dot{z}$  is a maximum when  $z$  is zero) is equal to the maximum potential energy ( $z$  is a maximum when  $\dot{z}$  is zero).

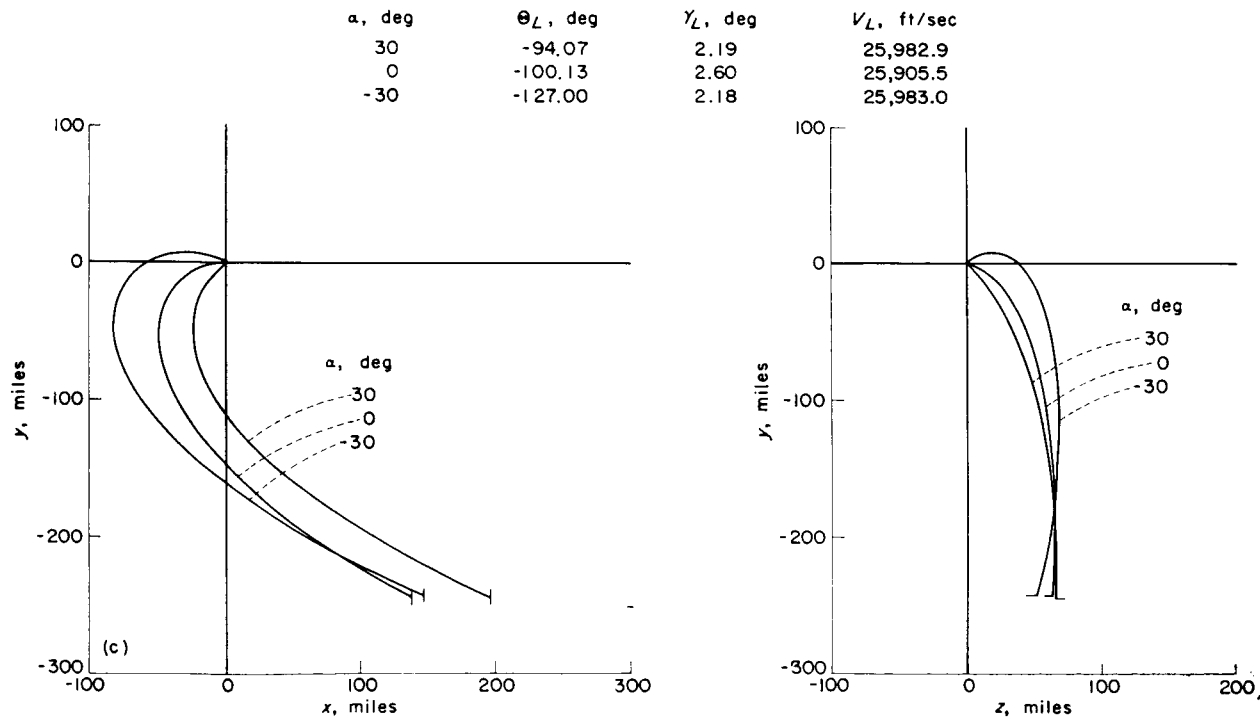
In the second example considered, the in-plane velocity was 600 feet per second and the out-of-

plane velocity was 200 feet per second. These trajectories are shown in figure 11(b) for values of  $\alpha$  of  $30^\circ$ ,  $0^\circ$ , and  $-30^\circ$ . Similar trajectories are shown in figure 11(c) where the out-of-plane velocity was 400 feet per second. A case was also calculated where the in-plane velocity was 800 feet per second and the out-of-plane velocity was 200 feet per second and this case is shown in figure 11(d). It may be seen in each of these cases that the aforementioned approximate relationship between  $z_{\max}$  and  $\dot{z}_0$  is valid for the selected range of values of the in-plane component of the closing velocity  $\Delta V \cos \beta$ . For each of these trajectories the angular distance traveled by the station, the launch velocity, and flight-path angle have been recorded in the figure. The reader should be cautioned, however, against a close comparison of these numbers with those given in figure 9, since in both instances the numbers were obtained by interpolating between numerical data points.



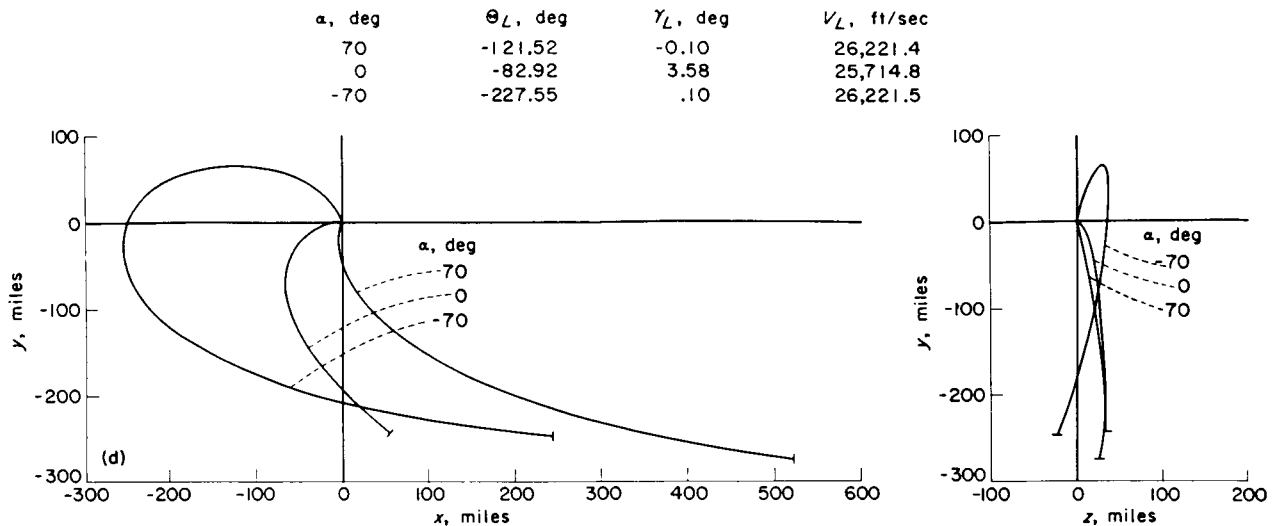
(b)  $\Delta V = 632.5$  feet per second;  $\beta = 18.4^\circ$  ( $\Delta V \cos \beta = 600$  feet per second;  $\Delta V \sin \beta = 200$  feet per second).

FIGURE 11.—Continued.



(c)  $\Delta V = 721.1$  feet per second;  $\beta = 33.7^\circ$  ( $\Delta V \cos \beta = 600$  feet per second;  $\Delta V \sin \beta = 400$  feet per second).

FIGURE 11.—Continued.

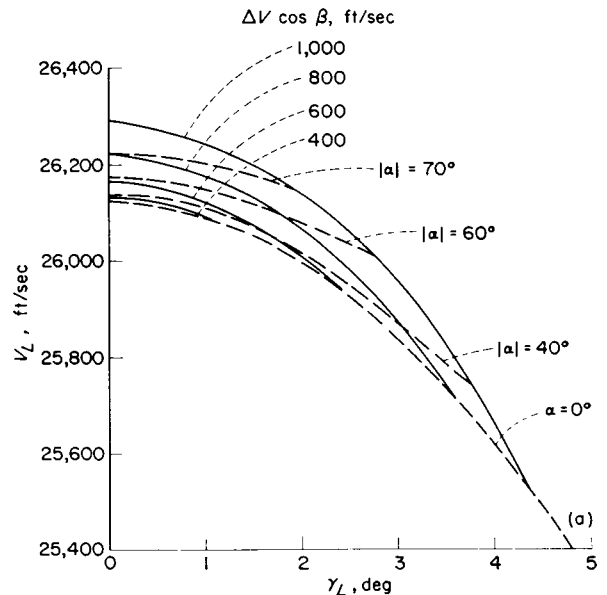


(d)  $\Delta V = 824.6$  feet per second;  $\beta = 14.0^\circ$  ( $\Delta V \cos \beta = 800$  feet per second;  $\Delta V \sin \beta = 200$  feet per second).

FIGURE 11.—Concluded.

**Boundaries of launch and rendezvous conditions.**—In the discussion of the foregoing trajectories, it was noted that, under certain launch conditions and along certain trajectories, rendezvous could be achieved with a station in a 300-mile circular orbit. With the orbit of the station and the launch altitude specified, the conditions at launch and at rendezvous will lie within certain definite boundaries. There are a number of ways of plotting such boundaries. If one considers the in-plane and out-of-plane motions as being independent and their effects additive, the boundaries of launch and rendezvous conditions may be plotted as a function of the angle of closure  $\alpha$ . Also of interest is the range of launch velocity and flight-path angle commensurate with a given closing velocity. Plots illustrating these variations are given in figure 12.

If a limiting value of in-plane closing velocity  $\Delta V \cos \beta$  is specified, the range of conditions at launch ( $V_L$  and  $\gamma_L$ ) which will achieve rendezvous without exceeding the selected limiting value of closing velocity may be obtained from figure 12(a). The region of possible launch conditions is represented by a half-crescent-shaped area defined by the three lines: the specified maximum allowable value of  $\Delta V \cos \beta$ , the axis  $\gamma_L = 0^\circ$ , and the line  $\alpha = 0^\circ$ . Also plotted in figure 12(a) are lines showing the angle of closure  $\alpha$  corresponding to the various combinations of permissible launch conditions. Positive values of  $\alpha$  result when



(a) Variation of the launch conditions showing lines of constant in-plane closing velocity and lines of constant in-plane closing angle.

FIGURE 12.—Boundaries of ferry launch and rendezvous conditions for the case of a station in a 300-mile circular orbit. Launch refers to the condition of boost burnout, which is assumed to be 60 miles above the surface of the earth.

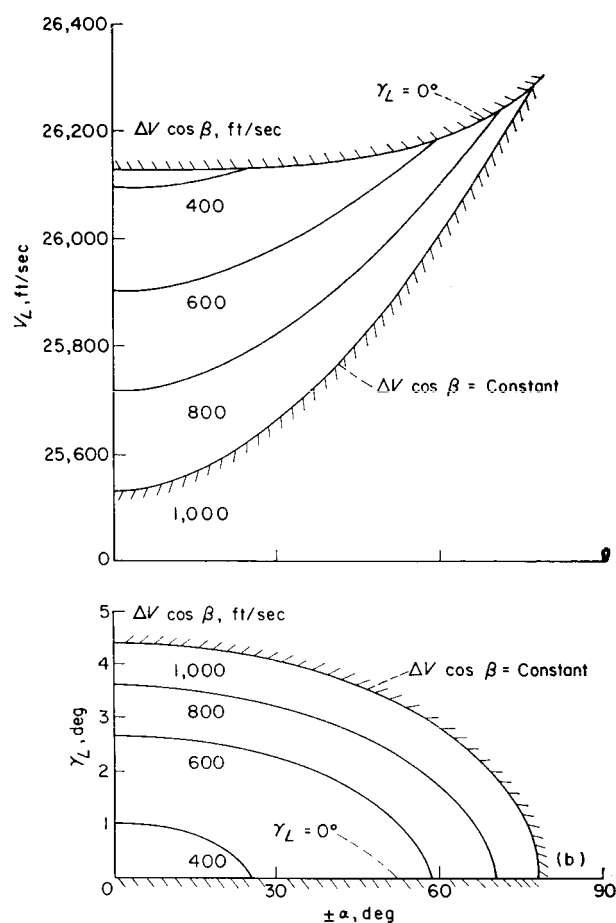
rendezvous is achieved in the ascending phase of the transfer trajectory (see fig. 1); negative values are associated with rendezvous in the descending phase.

The line  $\alpha=0^\circ$  is not a physical boundary but rather a line of symmetry. The two physical boundaries are lines of constant  $\Delta V \cos \beta$  and the line of  $\gamma_L=0^\circ$ . The maximum allowable  $\Delta V \cos \beta$  is a measure of the maximum fuel carried by the ferry for injection into orbit. The region  $\gamma_L < 0^\circ$  is excluded since a ferry launched at 60 miles with a sufficiently small negative flight-path angle would reach a perigee within the atmosphere and again pass through the 60-mile altitude with a positive flight-path angle. It is this positive flight-path angle and the associated velocity which must fall within the specified boundary. (If the launch altitude were sufficiently large so that drag could be ignored, the magnitudes of  $\gamma$  and of  $V$  would be unchanged and  $\gamma_L=0^\circ$  could be treated as a line of symmetry. The launch times, however, would be different.)

Figure 12(a) also illustrates that, if one specifies the (circular) orbit of the station and then specifies two of the variables, for example,  $V_L$  and  $\gamma_L$ , the trajectory conditions of the ferry as it passes through the orbital altitude of the station are fixed. (The quantities  $\Delta V$  and  $\alpha$  will be significant only if the station happens to be at the intersection of the orbits at that time.) Because of this restriction, the relative position of the two bodies at the time of launch is a dependent variable and cannot be independently chosen. Thus, there are only two independent variables to the problem once the station's orbit is established. However, those two variables do not have to be  $V_L$  and  $\gamma_L$ . For launch guidance one may prefer to specify a maximum value of  $\Delta V$  and a measured position of the ferry and then adjust the burnout conditions of the boost vehicle to satisfy the rendezvous conditions.

The effects of time on the launch conditions are covered in a subsequent section. Although figure 12(a) shows the necessary launch and corresponding rendezvous conditions jointly, additional insight into the boundaries may be obtained by cross plotting several of the variables. (See figs. 12(b) and 12(c).)

In figure 12(b), the launch velocity and flight-path angle are plotted as a function of the angle of closure  $\alpha$ . The boundaries of acceptable launch conditions lie between the line  $\gamma_L=0^\circ$  and the maximum allowable value of  $\Delta V \cos \beta$ . Only half the boundaries are shown since  $\pm\alpha$  is plotted on the abscissa. The contours indicate that, for a

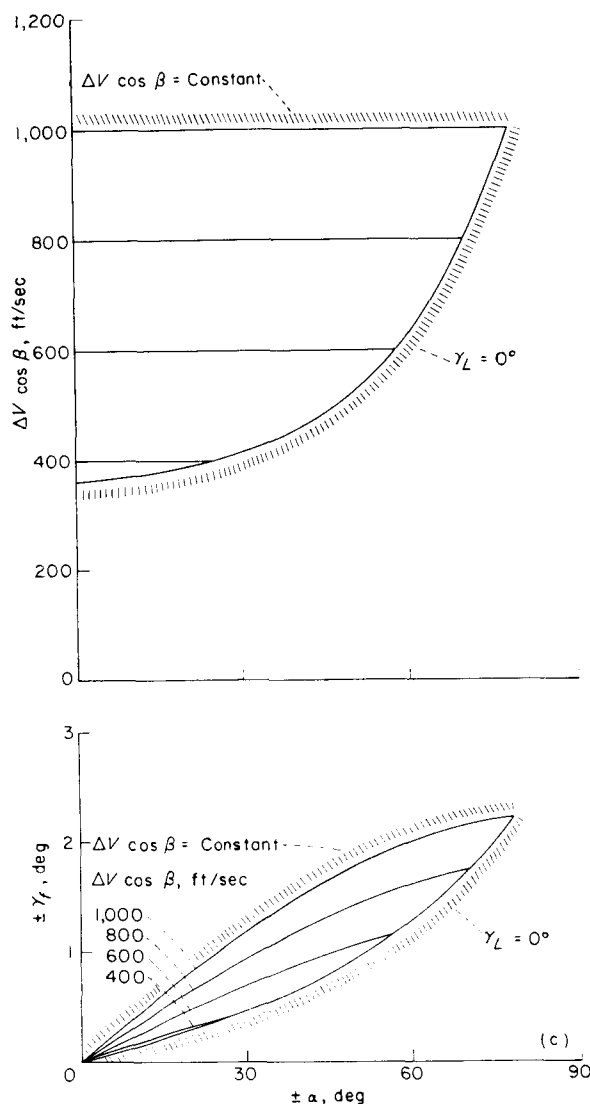


(b) Boundaries of inertial velocity and flight-path angle of ferry at time of launch as required for rendezvous.

FIGURE 12.—Continued.

given value of the in-plane closing velocity  $\Delta V \cos \beta$ ,  $V_L$  is a minimum and  $\gamma_L$  is a maximum at  $\alpha=0^\circ$ . As  $|\alpha|$  is increased,  $V_L$  increases and  $|\gamma_L|$  decreases.

In figure 12(c) the relative in-plane closing velocity and the ferry flight-path angle  $\gamma_f$  at rendezvous are plotted as functions of  $\alpha$ . Again the appropriate boundaries or contours are marked. The variation of  $\Delta V \cos \beta$  with  $\alpha$  is symmetric about the line  $\alpha=0^\circ$  while the variation of  $\gamma_f$  with  $\alpha$  is antisymmetric (positive  $\gamma_f$  with positive  $\alpha$ ). These boundaries show that, for a relative in-plane closing velocity of 400 feet per second, the angle of closure must lie between  $\pm 25^\circ$  and the  $|\gamma_f|$  must lie in a very narrow corridor between  $0.38^\circ$  and  $1.0^\circ$ . At a relative closing velocity of 1,000 feet per second, the relative angle of closure may be as much as  $\pm 78^\circ$  and the flight-path angle may be as much as  $\pm 2.23^\circ$ .



(c) Boundaries of the relative closing velocity and flight-path angle of the ferry at the time of rendezvous.

FIGURE 12.—Concluded.

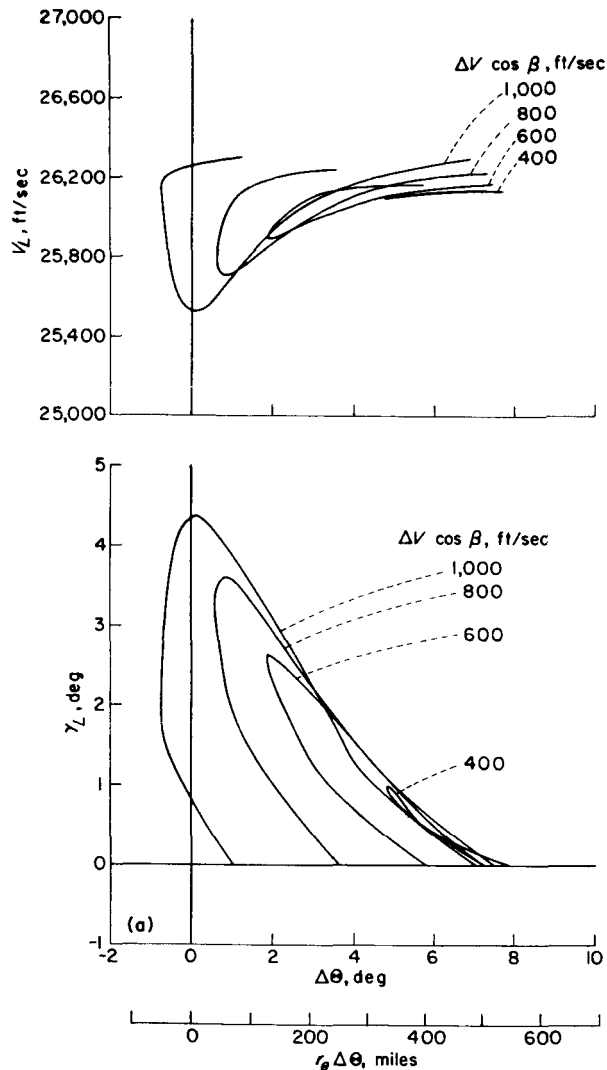
The boundaries given in figure 12 were obtained from two sources: the trajectories computed by the equations of motion of appendix A and the well-known closed-form solutions to Kepler's equations. The results obtained by the two methods were checked, one against the other, for possible errors. Since similar boundaries for any specified orbit may be computed with fairly simple equations, these equations and the considerations employed in their development are given in appendix D. It should be noted that these calculated boundaries do not involve the out-of-plane component of the closing velocity nor do they

involve the position and velocity as a function of time. For instance, the relative positions of the station and the ferry at any given time cannot be calculated in closed form.

#### Variation of conditions with launch time.—

For any given position of the space station with respect to the ferry at the time of booster burnout, the inertial velocity and flight-path angle of the ferry become uniquely specified if rendezvous or near rendezvous is to be accomplished with only small midcourse velocity corrections. For each second of delay in the time of firing of the booster on the ground, the station in a near-earth orbit will change its position by about 5 miles. Therefore, it appears certain that the conditions at the time of booster burnout must be varied to compensate for any delay in time. Such corrections could be fed into the booster guidance system right up to the instant of ground firing. Figure 13 shows the manner in which these conditions might vary for the case where the station is in a 300-mile circular orbit. Shown in figure 13(a) is the variation of ferry launch velocity and flight-path angle with respect to the angular separation between the space station and the ferry for different values of the in-plane closing velocity,  $\Delta V \cos \beta$ . The separation angle  $\Delta \theta$  is positive when the station is ahead of the ferry. (See appendix C.) The abscissa is also marked in terms of  $r_e \Delta \theta$  which is the separation distance between the ferry and the space station measured in statute miles on the surface of the earth. It may be seen that, with each increase in  $\Delta V \cos \beta$  (over the range investigated), somewhat larger values of separation distance or delayed times in launch may be accounted for. Also, if launch is attempted at the earliest possible time and the in-plane closing velocity is limited to 800 feet per second, the separation distance can decrease from 500 miles to 50 miles, and thus delays on the order of 90 seconds may be accounted for.

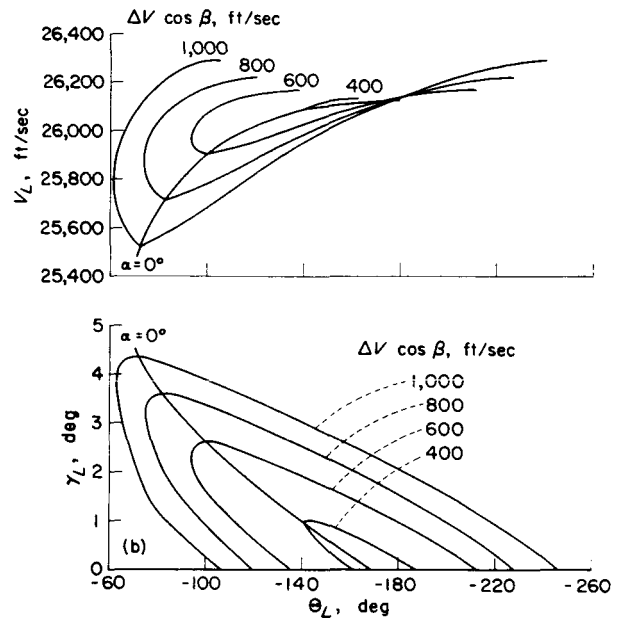
Depending upon when the vehicle is launched, rendezvous may occur from one-quarter to three-quarters around the earth from the launch position. The plots of figure 13(b) show the variation in the distance traveled around the earth from launch to rendezvous for certain specified rendezvous conditions. In figure 13(b) are the values of velocity and flight-path angle of the ferry plotted against  $\theta_L$  (that is, the position of the station at the time of booster burnout). Since at



(a) Relative position between ferry and station at launch.

FIGURE 13.—Variation of the launch velocity and flight-path angle of the ferry as a function of the relative and absolute positions of the station and ferry at the time of booster burnout. The variations are shown for several values of the closing velocity.

rendezvous  $\Theta=0^\circ$ , negative values of  $\Theta_L$  are shown. Contours have been drawn for launch conditions leading to rendezvous at specified values of the closing velocity  $\Delta V \cos \beta$ . As previously shown in figure 12, for each closing velocity there is a minimum launch velocity which is associated with the angle of closure  $\alpha=0^\circ$ . Contours through these minimum points have been drawn and are indicated on the figure as  $\alpha=0^\circ$ . The solid line, marked  $\alpha=0^\circ$ , gives the value of  $\Theta$  of the station at the time of ferry



(b) Absolute position of station at launch.

FIGURE 13.—Concluded.

launch. The figure shows, for example, that, with a closing velocity of 1,000 feet per second, the station is intercepted anywhere from  $63^\circ$  to  $246^\circ$  around the earth from its position at ferry launch depending on the launch conditions. For a minimum launch velocity of 25,525 feet per second, rendezvous will occur about  $73^\circ$  around the earth from the launch point and at rendezvous  $\alpha=0^\circ$ .

#### STATION IN AN ELLIPTIC ORBIT

**Trajectories.**—A limited number of rendezvous trajectories were calculated for a station in an elliptic orbit. In order to have some basis of comparison with a 300-mile circular orbit, the elliptic orbit was chosen to have a perigee at 100 miles and an apogee at 500 miles. The two orbits are illustrated in figure 14.

Rendezvous was investigated at four positions along the elliptic orbit: at perigee ( $\Theta=0^\circ$ ), at apogee ( $\Theta=180^\circ$ ), and at the intersection of the orbit with the latus rectum ( $\Theta=90^\circ, 270^\circ$ ). These rendezvous positions are also illustrated in figure 14. It was assumed that at rendezvous the out-of-plane velocity was 400 feet per second and the in-plane velocity was 600 feet per second for a total  $\Delta V$  of 721 feet per second. For all cases then,  $\beta$  was  $33.69^\circ$ . The in-plane angle of closure  $\alpha$  was varied from zero in both negative

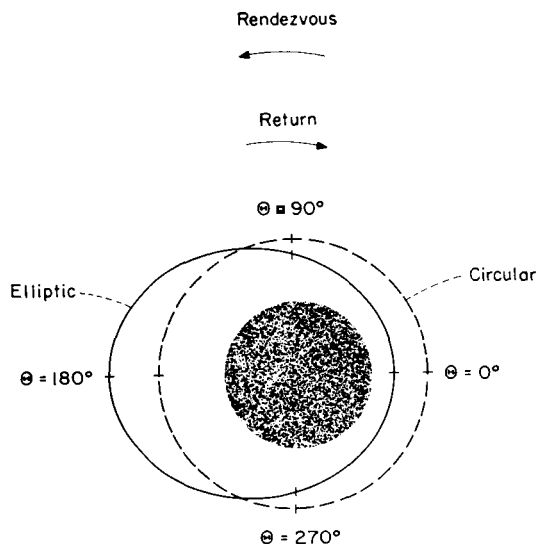


FIGURE 14.—Circular and elliptic orbits.

and positive directions until (in general) a value was reached where a launch from an altitude of 60 miles was not possible. The results of these calculations are shown in figures 15 to 18.

The inertial velocity of the station at the perigee of its orbit is 26,220.47 feet per second. The apogee velocity of a ferry on a trajectory whose perigee is 60 miles and whose apogee is 100 miles above the earth is 25,562.25 feet per second. Thus, the minimum closing velocity of the ferry and station at the station's perigee is 658.22 feet per second. Therefore, when rendezvous at the station's perigee with a closing velocity of 600 feet per second was considered, none of the trajectories satisfied the required launch conditions  $h_f = 60$  miles. However, a number of trajectories are shown in figure 15 for cases where  $\alpha$  varied from  $50^\circ$  to  $-50^\circ$ . Shown on the (a), (b), and (c) parts of figure 15 are the  $y, x$  variation, the  $y, z$  variation, and the  $\dot{R}, R$  variation, respectively. Listed in a table in the figure is the minimum altitude reached

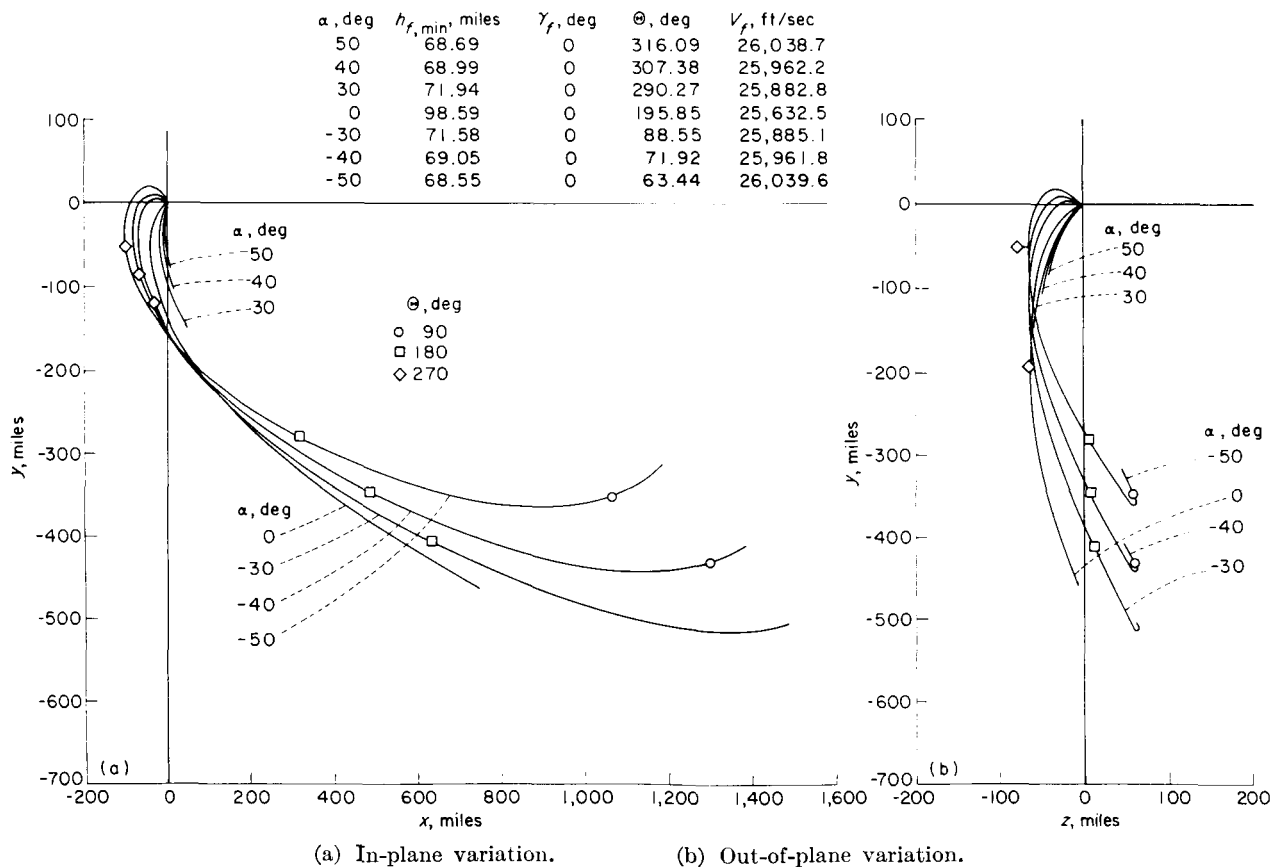


FIGURE 15.—Trajectories of a ferry vehicle during rendezvous with a station in a 100- to 500-mile elliptic orbit. Rendezvous occurs at  $\Theta = 0^\circ$  (perigee).  $\Delta V \cos \beta = 600$  feet per second.



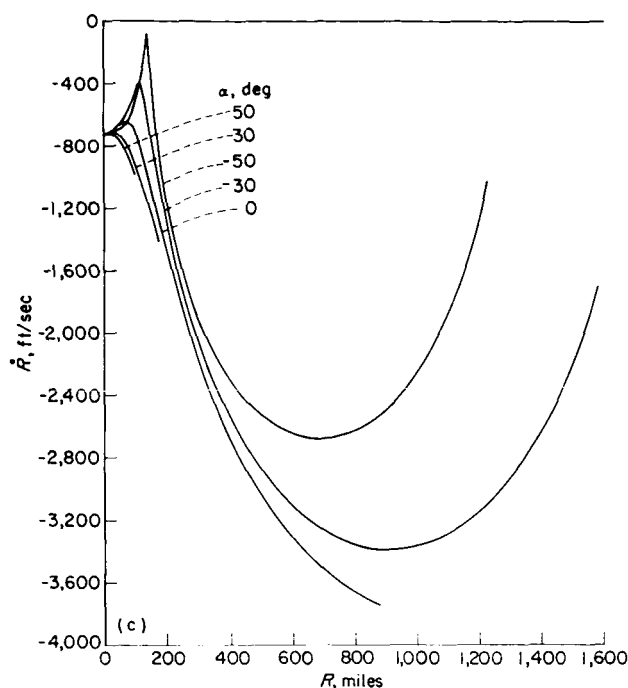


FIGURE 15.—Concluded.

by the ferry  $h_{f,min}$  (perigee), the  $\theta$  position of the station, and the inertial velocity of the ferry at this condition. Each of these trajectories was terminated when the ferry was at the minimum altitude. In order to facilitate a study of these trajectories, most trajectories have been marked by a symbol when the station is at  $270^\circ$ ,  $180^\circ$ , and  $90^\circ$ . Whenever the trajectories could not be marked clearly, no mark was used.

In figure 16 are shown the trajectories obtained for the ferry vehicle when rendezvous occurred at  $\theta=90^\circ$ . All the trajectories shown are possible rendezvous trajectories and ticks have been put at the end of each trajectory to denote this fact. The conditions at launch for each trajectory are tabulated in the figure. It may be seen that  $\alpha$  varied from  $-60^\circ$  to  $100^\circ$ . The lack of symmetry in the range of  $\alpha$  is due to the fact that the inertial velocity of the station is not aligned with the  $X$ -axis of the station at the time of rendezvous.

Figure 17 shows all the trajectories obtained when rendezvous occurred at  $\theta=180^\circ$ . At apogee, the inertial velocity of the station was 23,868.79 feet per second while a ferry on a 60- to 500-mile orbit will have an inertial velocity of 23,806.80 feet per second at this point. Thus, a minimum relative closing velocity of about 62

feet per second is theoretically possible. For the specified in-plane closing velocity of 600 feet per second, the spread in the available  $\alpha$  range for rendezvous is somewhere between  $\pm 80^\circ$  and  $\pm 90^\circ$ . Symmetry occurs because the inertial velocity of the station and the  $X$ -axis are again colinear at rendezvous. The launch conditions are tabulated in the figure for each trajectory shown. Symbols are placed on most of the trajectories to indicate the point at which  $\theta$  was  $90^\circ$ .

In figure 18 the trajectories which led to rendezvous at  $\theta=270^\circ$  are shown. The trajectories are again marked in the same fashion as shown in figures 16 and 17. Symbols are used to indicate the position of the ferry when the station was at  $\theta$  of  $180^\circ$  and  $90^\circ$ . In this case  $\alpha$  varied from  $60^\circ$  to  $-100^\circ$ .

It is interesting to note that the maximum available spread in  $\alpha$  is almost identical for rendezvous at  $\theta$  of  $90^\circ$ ,  $180^\circ$ , and  $270^\circ$ . In each of these cases  $\alpha$  varied through about  $160^\circ$ . This result was surprising in that it was thought that the spread in  $\alpha$  at  $\theta=180^\circ$  would be notably larger than that at  $\theta$  of  $90^\circ$  and  $270^\circ$ .

Considered individually, the trajectories leading to rendezvous with a station in an elliptic orbit are very similar to those obtained when the station was in a circular orbit. However, if considered as families of trajectories, the families are markedly different. One difference is primarily due to the fact that both the altitude and angular velocity of the rotating coordinate system are going through a nearly sinusoidal, rather than a constant, variation with time. In figures 16, 17, and 18, it may be noted that, if a line were drawn connecting the launch points of each of the trajectories, it would have a cycloidal character. With the station in a circular orbit this locus of launch positions was an arc of a circle of radius 4,020 statute miles. (See fig. 9.)

The 400-feet-per-second out-of-plane velocity component again produced a lateral displacement of the ferry of about  $70 \pm 3$  miles. It should be noted, however, that, when rendezvous occurred at  $\theta=90^\circ$ , the launch position was less than a quarter of the way around the earth and the lateral range of less than 70 miles is obtained. This condition implies that for these cases the out-of-plane velocity of more than 400 feet per second must be used if a lateral displacement of 70 miles is required.

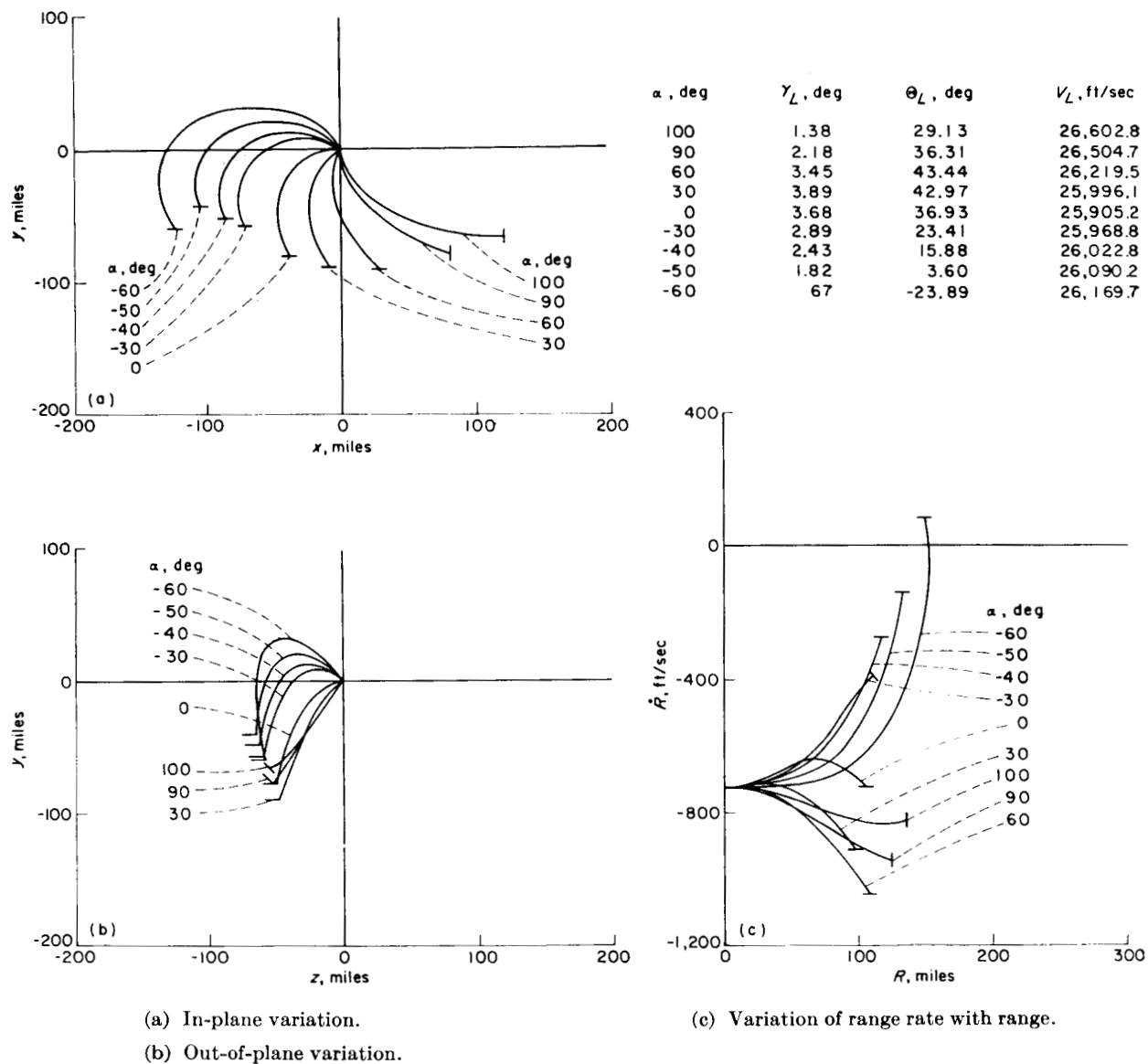
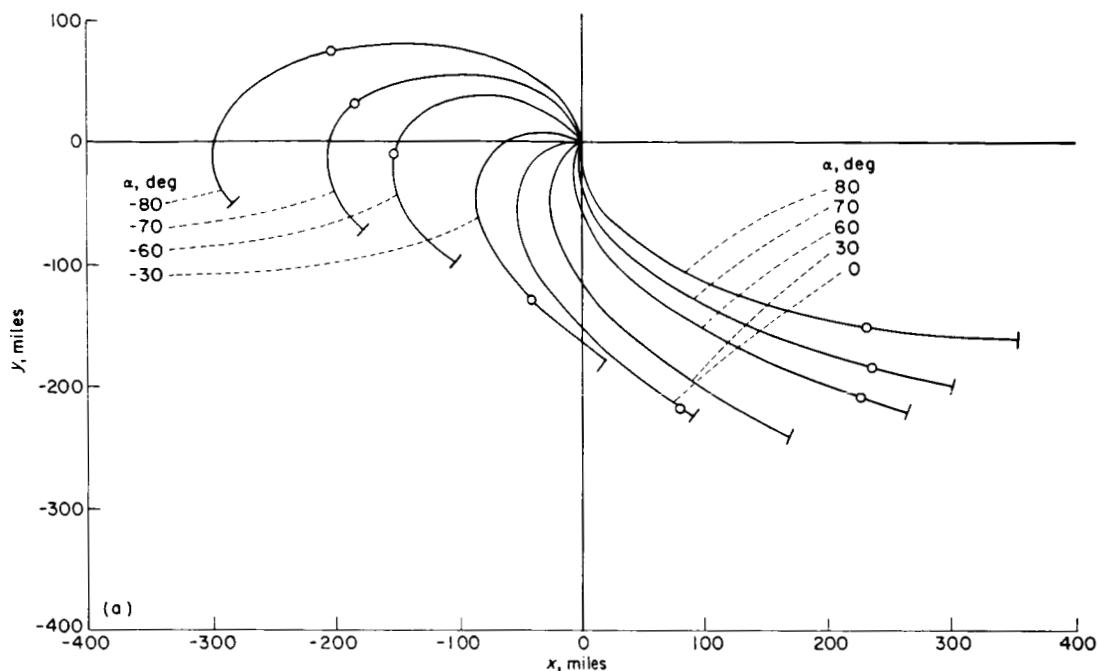
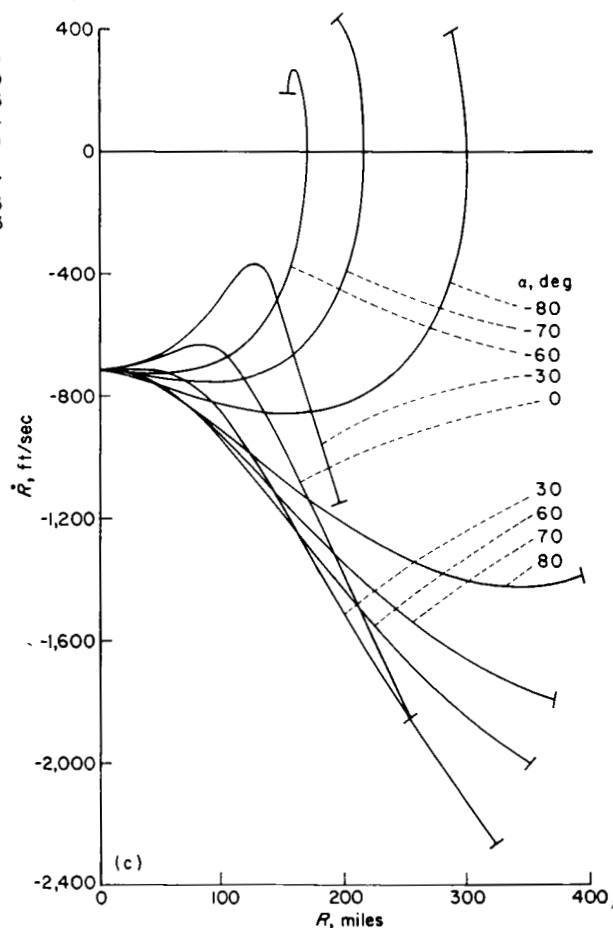
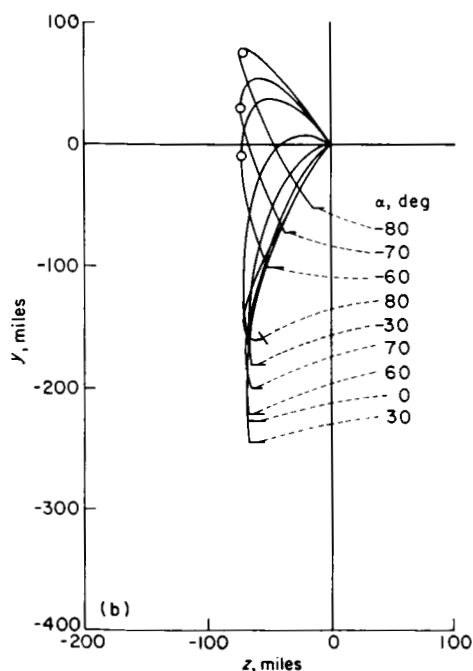


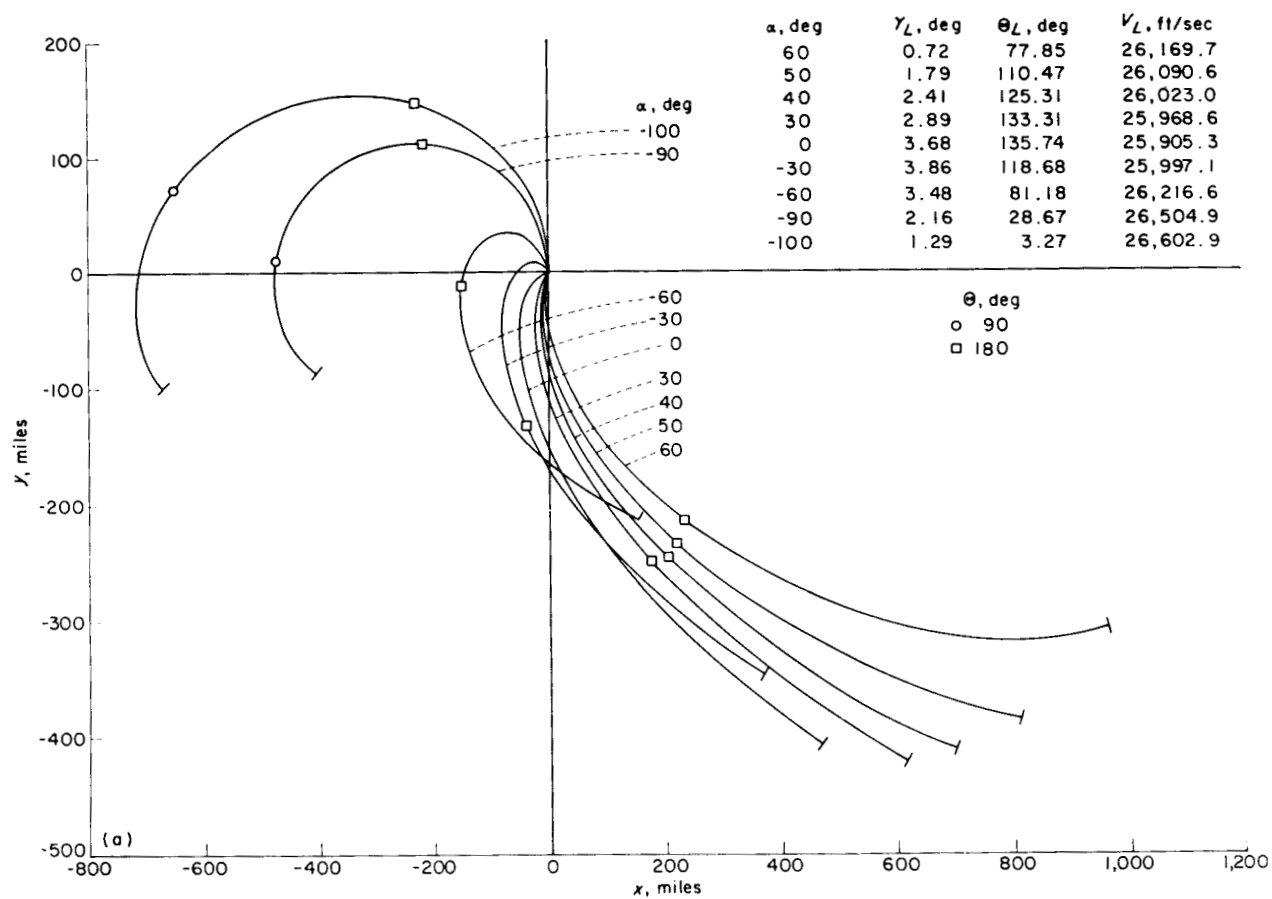
FIGURE 16.—Trajectories of a ferry vehicle during rendezvous with a station in a 100- to 500-mile elliptic orbit. Rendezvous occurs at  $\theta = 90^\circ$ ;  $\Delta V \cos \beta = 600$  feet per second.



$\alpha$ , deg	$\gamma_L$ , deg	$\Theta_L$ , deg	$V_L$ , ft/sec
80	1.85	62.98	26,384.5
70	2.91	77.05	26,293.0
60	3.65	84.48	26,207.3
30	4.91	92.01	26,007.4
0	5.33	88.15	25,931.9
-30	4.91	74.70	26,007.1
-60	3.63	46.71	26,207.7
-70	2.92	31.13	26,293.3
-80	1.88	8.29	26,384.3

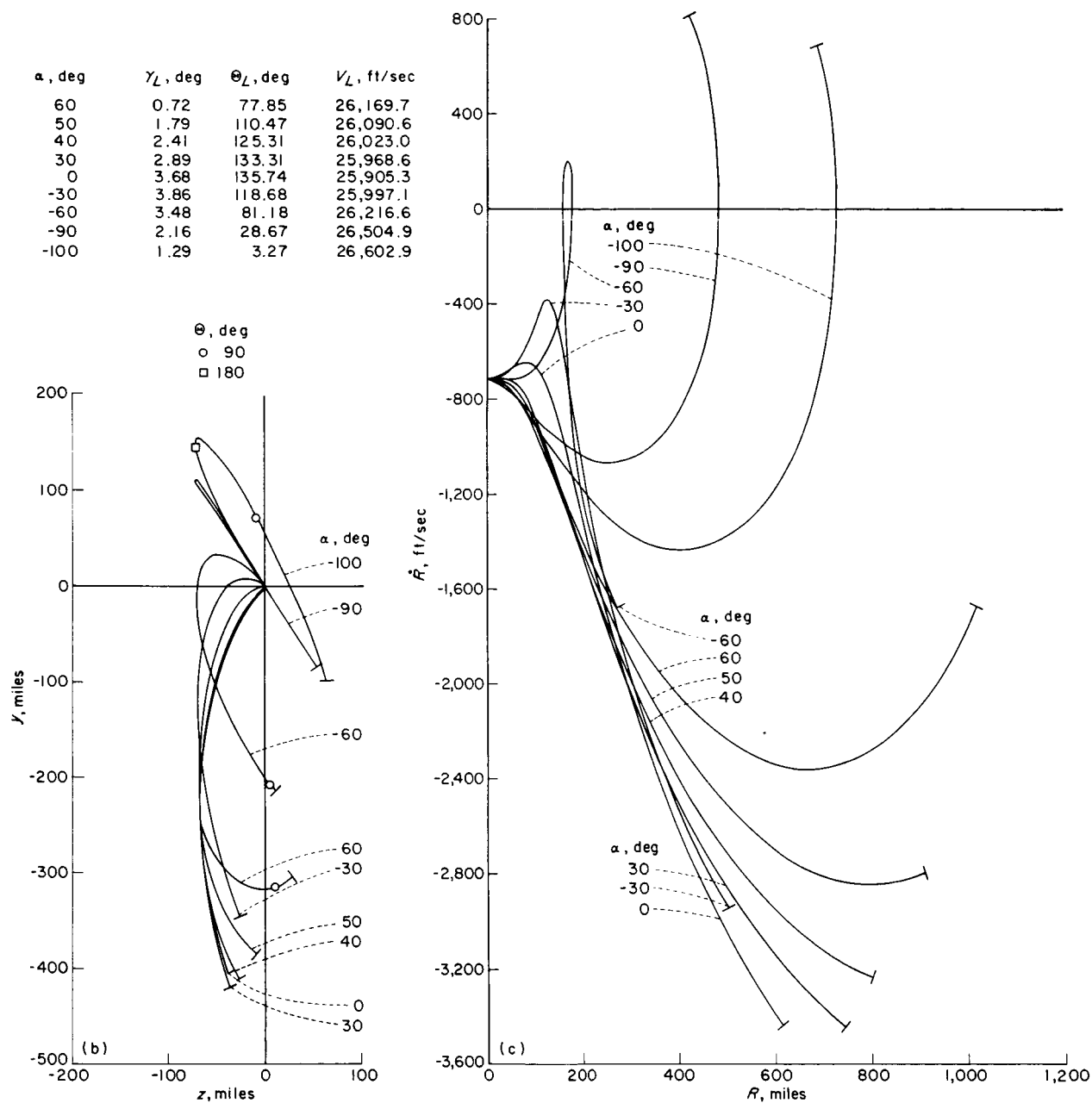


(a) In-plane variation. (b) Out-of-plane variation. (c) Variation of range rate with range.  
 FIGURE 17.—Trajectories of a ferry vehicle during rendezvous with a station in a 100- to 500-mile elliptic orbit.  
 Rendezvous occurs at  $\Theta = 180^\circ$  (apogee).  $\Delta V \cos \beta = 600$  feet per second.



(a) In-plane variation.

FIGURE 18.—Trajectories of a ferry vehicle during rendezvous with a station in a 100- to 500-mile elliptic orbit. Rendezvous occurs at a  $\theta=270^\circ$ .  $\Delta V \cos \beta=600$  feet per second.



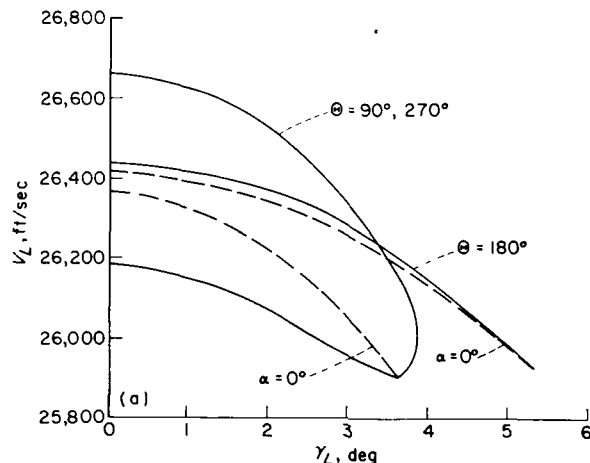
(b) Out-of-plane variation. (c) Variation of range rate with range.

FIGURE 18.—Concluded.

**Boundaries of launch and rendezvous conditions.**—The results of figures 15 to 18 and the equations of appendix D have been used to summarize boundaries of launch and rendezvous conditions for the case where a station is in a 100- to 500-mile elliptic orbit. These boundaries are shown in figure 19. In figure 19(a) the range of possible launch conditions is shown for rendezvous with an in-plane velocity component of 600 feet per second. Also shown in figure 19(a) are the variations of launch conditions when the closing velocity is varied but the angle of closure  $\alpha$  is held constant at zero. Note that for rendezvous at  $\Theta=90^\circ$  and  $270^\circ$  that the  $\alpha=0^\circ$  line lies within the boundary.

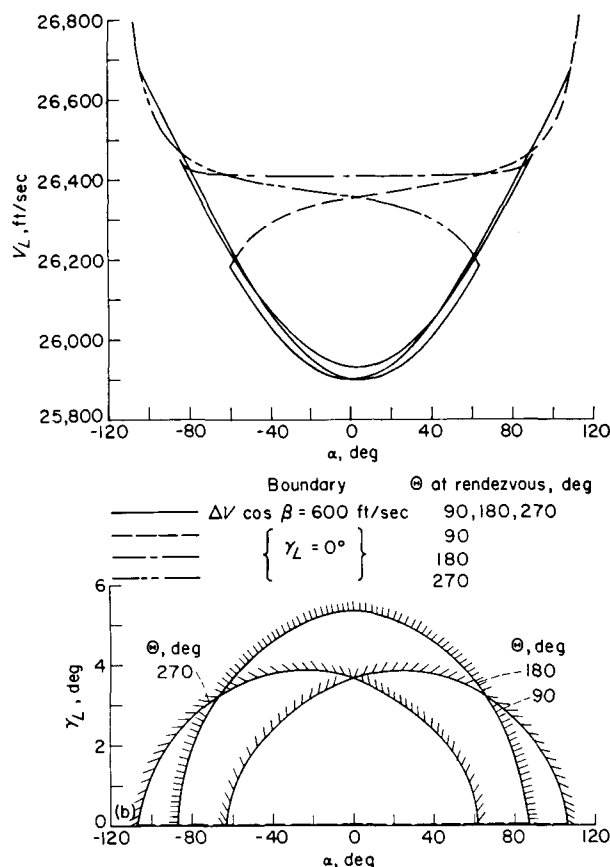
In figure 19(b) the boundaries of the conditions at launch are shown in terms of  $V_L$  and  $\gamma_L$  of the ferry plotted against the angle of closure  $\alpha$ . In figure 19(c) the boundaries of rendezvous conditions,  $\Delta V \cos \beta$  and  $\gamma_f$  for the ferry are shown. In all but one case the boundaries are shown for rendezvous at  $\Theta=90^\circ$ ,  $180^\circ$  and  $270^\circ$  only. The one exception is in figure 19(c) in the variation of  $\Delta V \cos \beta$  with  $\alpha$  for the case of  $\Theta=0^\circ$  (or  $360^\circ$ ). It may be seen that this contour does not intersect the line for  $\Delta V \cos \beta=600$  feet per second.

Parallel to the presentation made in figure 10, the boundaries of figure 19 are given in terms of the in-plane closing velocity with the assumption that



(a) Variations of the launch conditions showing lines of  $\alpha=0^\circ$  and  $\Delta V \cos \beta=600$  feet per second.

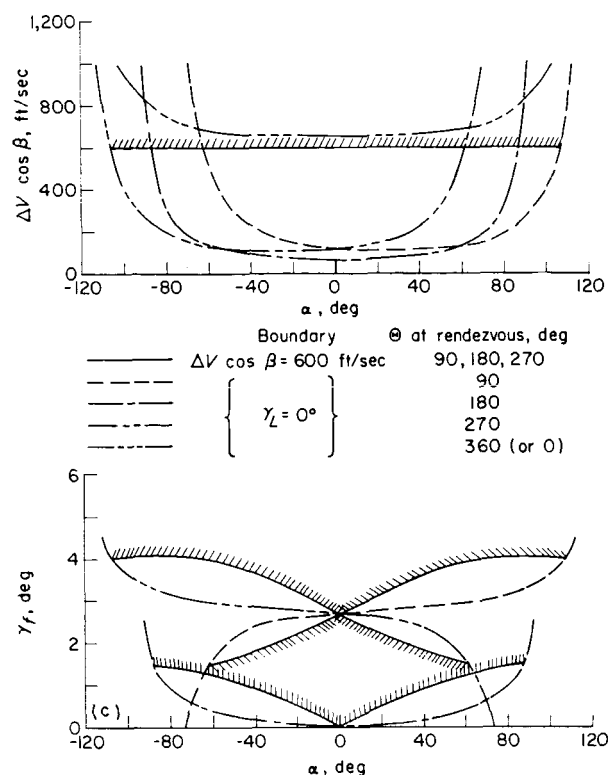
FIGURE 19.—Envelopes of ferry launch and rendezvous conditions for case of the station in a 100- to 500-mile elliptic orbit. Envelopes are shown for rendezvous at  $\Theta=90^\circ$ ,  $180^\circ$ , and  $270^\circ$  for in-plane closing velocities of 600 feet per second or less and for  $\gamma_L \geq 0^\circ$ .



(b) Boundaries of launch conditions as a function of the angle of closure  $\alpha$ .

FIGURE 19.—Continued.

the results were not dependent on the out-of-plane velocity. With the station in a circular orbit, this assumption was justified by showing that the in-plane and out-of-plane motions were virtually independent and could be treated separately. This condition has also been verified in the present case. A comparison was made of the results taken from figure 18 (with an out-of-plane velocity of 400 feet per second) with those calculated with a zero out-of-plane velocity and with boundaries calculated by the method of appendix D. (In-plane considerations only were used.) Virtually no difference could be detected in the launch conditions. This fact can be appreciated by noting that the vector addition of a 400-foot-per-second velocity component normal to a 25,000-foot-per-second component produces an increase in velocity of about 3 feet per second. Thus, within the reading accuracy the plots of figure 19 may be applied to out-of-plane trajectories, but caution



(c) Boundaries of rendezvous conditions as a function of the angle of closure  $\alpha$ .

FIGURE 19.—Concluded.

should be used if  $\beta > 60^\circ$ .

In figure 19, the acceptable range of variables again lies between boundaries defined by the contours for  $\gamma_L = 0^\circ$  and the maximum acceptable (in-plane) closing velocity, arbitrarily taken to be 600 feet per second. In figure 19(c) the  $\gamma_L = 0^\circ$  contours have been extended out to the condition where  $\Delta V \cos \beta = 1,000$  feet per second in order to show the extreme sensitivity of this contour at the larger values of closing velocity. In figure 19(b) the hatching has been left off the  $\Delta V \cos \beta$  boundary of launch velocities for the sake of clarity.

Examination of the variations in these boundaries for rendezvous at the various positions of the station indicates that in the sector of the ellipse defined by  $270^\circ \geq \theta \geq 90^\circ$  (the apogee sector):

(1) The minimum values of launch and closing velocity do not vary greatly as  $\theta$  changes. These minimum values occur between values of  $\alpha$  of  $\pm 20^\circ$ .

(2) Relative velocity and flight-path angle at rendezvous change very little with  $\alpha$  over a range of about  $100^\circ$  (fig. 19(c)). At the extreme end of

the  $\alpha$  range, however, the variations of  $\Delta V \cos \beta$  and  $\gamma_f$  change very rapidly with small changes in  $\alpha$ .

(3) For a  $\Delta V \cos \beta \geq 200$  feet per second, the total range of  $\alpha$  available for rendezvous for any given value of closing velocity is about the same for any value of  $\theta$ .

(4) The boundary of launch conditions (fig. 19(a)) is very narrow for rendezvous at  $\theta = 180^\circ$  but opens up considerably for rendezvous at  $\theta = 90^\circ$  and  $270^\circ$ .

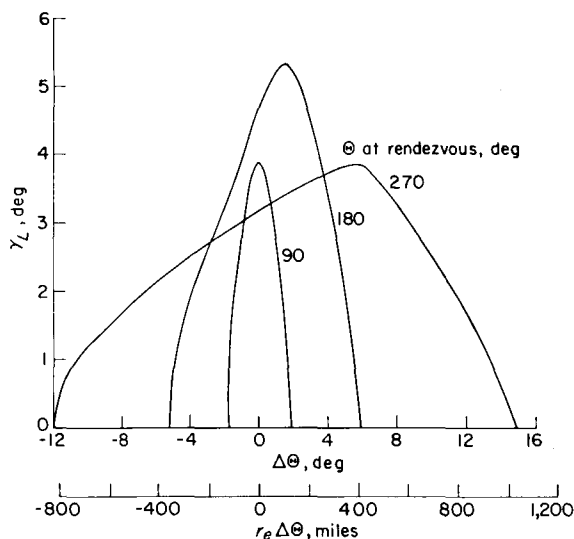
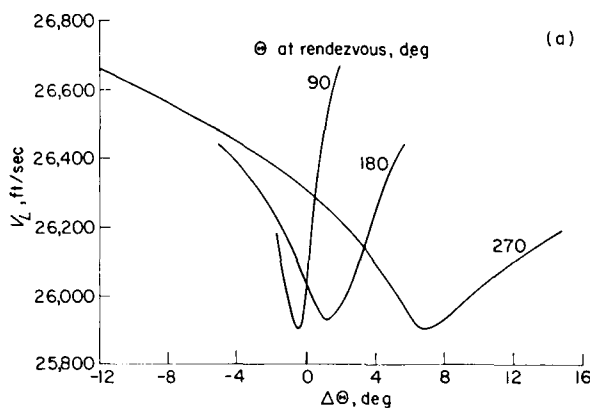
(5) With a maximum in-plane closing velocity component of 600 feet per second, the launch velocity may be reduced by as much as 500 feet per second below that required for a minimum closing velocity rendezvous. This result is similar to that noted for the case of the station in a circular orbit.

Very little advantage can be seen for rendezvous in the sector between  $270^\circ < \theta < 90^\circ$  (the perigee sector) since conditions are changing rapidly along that part of the orbit. It can, for example, be seen in figure 19(c) that the minimum in-plane closing velocity changes from 108 feet per second to 660 feet per second between the intersection with the latus rectum and perigee. However, it is interesting to note that the  $\gamma_L = 0^\circ$  boundary for rendezvous at perigee also exhibits the weak variation of  $\Delta V \cos \beta$  with  $\alpha$  displayed by the curves for rendezvous at the other three positions.

#### Variation of conditions with launch time.—

In the case of the station in a circular orbit, the variation of the launch conditions and the time available for launch were limited only by the desired closing velocity. The down-range position at which rendezvous was to occur was not important because there was only one possible orientation of the orbit of the station with respect to the circular earth. With the station in an elliptic orbit this limitation no longer exists. Because the station velocity and altitude are changing continuously, the orientation of the station's orbit and down-range position of the station at which rendezvous is to occur will directly affect the launch conditions. Although each position of the station is unique, the trend of the change in launch conditions with the value of  $\theta$  at rendezvous can be seen in figure 20.

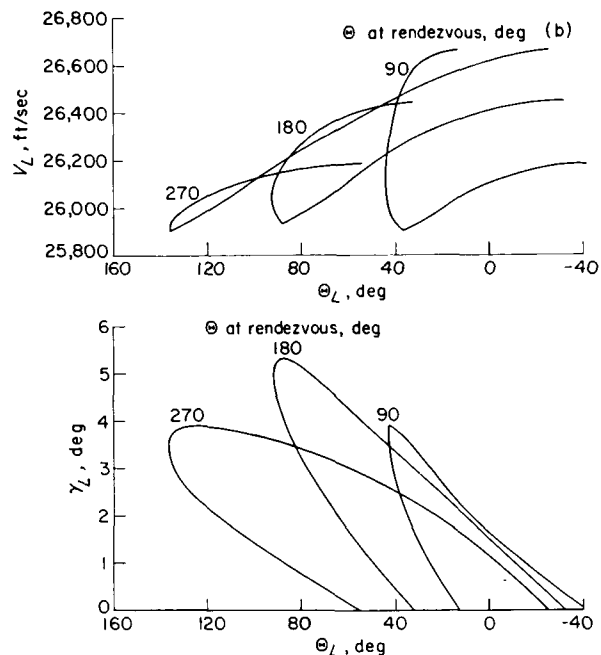
Figure 20(a) shows the relative position of the station and ferry at the time of ferry launch. The scales shown along the abscissa give both



(a) Boundaries of launch conditions as a function of the relative position of the ferry and station at launch,  $\Delta\Theta$  and  $r_e\Delta\Theta$ .

FIGURE 20.—Variation of launch velocity and flight-path angle for the ferry as a function of the absolute and relative positions of the station at launch. Contours represent a maximum in-plane closing velocity of 600 feet per second.

the separation angle measured from the center of the earth  $\Delta\Theta$  and the separation distance measured over the surface of the earth  $r_e\Delta\Theta$ . Positive values of  $\Delta\Theta$  are used when the station is ahead of the ferry at the time of launch. Figure 20(b) shows the absolute position of the station at the time of ferry launch when rendezvous is to occur at 600 feet per second at  $\Theta=90^\circ$ ,  $180^\circ$ , and  $270^\circ$ . The values of  $\Theta_L$  shown on the abscissa are in agreement with the definition of  $\Theta$  for an elliptic orbit; namely,  $\Theta_L=0^\circ$  means that the ferry launch occurred when the station was at the perigee of its orbit. It may be noted that



(b) Boundaries of launch conditions as a function of the absolute position of the station at launch  $\Theta_L$ .

FIGURE 20.—Concluded.

the curves of figure 20 are the contours for  $\Delta V=600$  feet per second of figure 19 and that the  $\gamma_L=0^\circ$  contours could be used to close the boundaries.

Figure 20(a) indicates that launch times are very limited if rendezvous is to be made at  $\Theta=90^\circ$ . For this case the station must be somewhere between 125 statute miles behind to 130 statute miles ahead of the ferry at the time of launch. This total spread of 255 statute miles is comparable to roughly 380 miles when the station is in a circular orbit, where in both cases the in-plane closing velocity is 600 feet per second. Rendezvous at  $\Theta=180^\circ$  and  $270^\circ$  offer a larger spread in launch time.

In figure 13(a) it was shown that, with the station in a 300-mile circular orbit, most of the possible launch conditions occurred with the ferry behind the station. For the station in a 100- to 500-mile elliptic orbit, figure 20(a) shows that the relative positions at launch are about equally divided between the ferry ahead of or behind the station.

Figure 20(b) shows that a rendezvous at  $\Theta=90^\circ$  can be obtained by launching from a position between  $\Theta=-41^\circ$  and  $44^\circ$  and that the launch velocity changes less than 300 feet per second between



the two extremes. Thus a rendezvous could occur at a position  $46^\circ$  ( $90^\circ - 44^\circ$ ) down range from the launch if all other conditions were met. Rendezvous at  $180^\circ$  and  $270^\circ$  positions require progressively longer down-range distances.

### DISCUSSION

In the foregoing sections, typical trajectories leading to rendezvous with a station in an elliptic and a circular orbit were illustrated. Boundaries which define the allowable launch and rendezvous conditions were also developed. There is, of course, nothing unique about the particular orbits chosen as examples. The range of allowable near-earth orbits is usually restricted to the region above the sensible atmosphere of the earth and below the Van Allen radiation belt. An altitude of 300 miles has often been considered a mean value for this region.

The trajectories were limited to those which produced a closing velocity at rendezvous of 1,000 feet per second or less. This limitation was imposed since, according to the formula for an impulsive velocity change

$$\frac{\Delta W}{W} = 1 - \exp\left(\frac{-\Delta V}{gI_{sp}}\right) \approx \frac{\Delta V}{gI_{sp}} \quad (2)$$

a  $\Delta V$  of 1,000 feet per second represents about 12.5 percent of the payload of the ferry ( $I_{sp}=250$  seconds). The results show, however, that this increase in the closing velocity is not entirely lost, since in most cases there is a reduction in the launch velocity. If the closing velocity is increased from the minimum of 360 feet per second to a value of 1,000 feet per second, the launch velocity may be reduced from a value of 26,125 feet per second to a value of 25,525 feet per second. (See fig. 10(b).) Thus, an increase in the relative velocity at rendezvous of 640 feet per second may be compensated by as much as a 600-foot-per-second reduction in launch velocity. This large reduction in launch velocity is, of course, realized only at one instant of launch time and any error in this launch time will lead to a requirement for somewhat larger launch velocities for the same closing velocity.

With reference to launch times, it is interesting to note in figure 13(a) that, regardless of the closing velocity, the station cannot be more than about 540 miles ahead of the ferry at the time of launch in order to achieve rendezvous in a 300-

mile circular orbit. Increasing the closing velocity allows the ferry to be launched at an earlier time but does not allow the ferry to be launched at a later time.

The results show that the out-of-plane motion of a ferry may be treated as virtually independent of the in-plane motions. If rendezvous is to occur after the ferry has passed more than a quarter of the way around the earth, the ferry may be launched in a direction parallel to the orbital plane of the station. At a point a quarter of the way around the earth, the ferry will pass through the plane of the station's orbit and an attempt should be made to bring the out-of-plane velocity  $\dot{z}$  to zero. The cost of this maneuver will be a function of the out-of-plane distance at launch and is given by equation (1). If rendezvous is to occur at a point less than a quarter of the way around the earth from launch, the ferry must have a  $\dot{z}$  component at launch sufficient to insure that the ferry will intersect the plane of the station's orbit before or at the time of rendezvous. One reason for this prior intersection, other than simplicity of injection guidance, is found in the fact that the inertial velocity of the ferry is lower before the ferry is injected into orbit than it is afterwards. Therefore, the out-of-plane velocity corrections will be smaller.

In the case where the station is in an elliptic orbit, it appears that the variation in the launch conditions could become very critical. The results of the one elliptic orbit considered indicate that perigee would be the least desirable position to attempt rendezvous and near apogee, the most desirable. Near apogee, the available launch time is relatively large, the required injection velocity is a minimum, and the conditions at rendezvous are relatively invariant with the angle of closure over a fairly wide range of conditions. Rendezvous between perigee ( $\theta=0^\circ$ ) and the ascending intersection with the latus rectum ( $\theta=90^\circ$ ) offers one advantage in the form of having the rendezvous occur relatively close to the launch site (on the order of  $45^\circ$  down range compared with  $90^\circ$  to  $180^\circ$  around the earth for rendezvous at apogee).

The choice of positions of the station at the time of rendezvous may, of course, be somewhat academic since in practice the orbit of the station must also pass relatively close (laterally) to the launch site at the time of launch. Thus, when the station is in an elliptic orbit, some compromise

may be necessary between an orbital pass that has favorable lateral characteristics and one that has favorable orientation characteristics. With a circular orbit, this orientation problem does not arise.

In programing the launch conditions to compensate for delays in launch time, rendezvous with a station in an elliptic orbit appears to be more difficult than that of a station in a circular orbit since the altitude, velocity, and down-range position of the station at which rendezvous is to occur are constantly changing with time. The results shown in figure 20 indicate that these changes are not severe for the example orbit but would probably become more severe as the eccentricity of the station's orbit is increased.

### CONCLUSIONS

It may be concluded that, for any orbit that a space station may have, there is a family of trajectories leaving the earth's atmosphere with different velocities and along different flight paths which, without further thrusting, will terminate at some instantaneous position of the station. These families may be computed and the launch conditions required for rendezvous determined. The equations and procedures have been developed for computing these trajectories and the proper launch conditions (at time of booster burnout).

Typical calculations have been performed for a station in a circular orbit 300 miles above the earth and for a station in an elliptic orbit having a perigee 100 miles and an apogee 500 miles above the earth. These numerical studies indicate that the launch velocity may be reduced as the closing velocity is increased but, in no case, is the sum of the two less

than that obtained for the Hohmann ellipse. As the allowable closing velocity is increased, the range of possible launch and rendezvous conditions increases and the time available for launch increases. If the closing velocity between the two vehicles at rendezvous is limited to about 500 feet per second above the minimum, rendezvous will generally occur with the station overtaking the ferry. However, with the station in an elliptic orbit, rendezvous can occur with the ferry overtaking the station from above or below. In either case the rate of closure approaches a constant and remains essentially constant during the last few minutes before rendezvous. This condition, which is indicative of a collision course, could provide a criterion for guidance during the terminal phase.

If the station is in an elliptic orbit, rendezvous appears to be more desirable near apogee than near perigee. Furthermore, it appears that launch guidance for rendezvous with a vehicle in an elliptic orbit will be more critical than that for one in a circular orbit; however, once launched, the range and variation of available rendezvous conditions make rendezvous with a station in an elliptic orbit more favorable if rendezvous is to occur somewhere near apogee. In either case, however, it appears that the prediction of desirable rendezvous trajectories is feasible and that launch and probably midcourse guidance will be necessary to allow for delays in launch time and to insure that the proper trajectory is established.

LANGLEY RESEARCH CENTER,  
NATIONAL AERONAUTICS AND SPACE ADMINISTRATION,  
LANGLEY FIELD, VA., October 27, 1960.

## APPENDIX A

### EQUATIONS OF MOTION OF A MASS AS MEASURED IN A ROTATING FRAME OF AXES WHICH FOLLOWS A KEPLERIAN TRAJECTORY

The method of Lagrange is employed in deriving the equations of motion based on the kinetic and potential energy of the mass at any instant. Sketch 1 shows the coordinates and the velocity

The velocity of the mass with respect to the center of the earth's gravitational field (taken as the absolute system) and with respect to the rotating  $x, y, z$  coordinate system is given by

$$\mathbf{V} = \frac{d\mathbf{r}_f}{dt} = \frac{d\mathbf{r}_s}{dt} + \frac{d'\mathbf{R}}{dt} + \boldsymbol{\Omega} \times \mathbf{R} \quad (\text{A2})$$

where the prime denotes the change as seen from the origin of the coordinate system. The vectors in equation (A2) have the components

$$\boldsymbol{\Omega} = (0, 0, \dot{\Theta})$$

$$\mathbf{R} = (x, y, z)$$

$$\mathbf{r}_f = (x, y + r_s, z)$$

$$\frac{d\mathbf{r}_s}{dt} = (-r_s \dot{\Theta}, \dot{r}_s, 0)$$

where  $r_s$  and  $\dot{\Theta}$  are not coordinates of the mass but are specified time-dependent parameters. The absolute velocity of the mass in terms of the coordinates  $x, y, z$ , and the parameters  $r_s, \dot{\Theta}$  is then

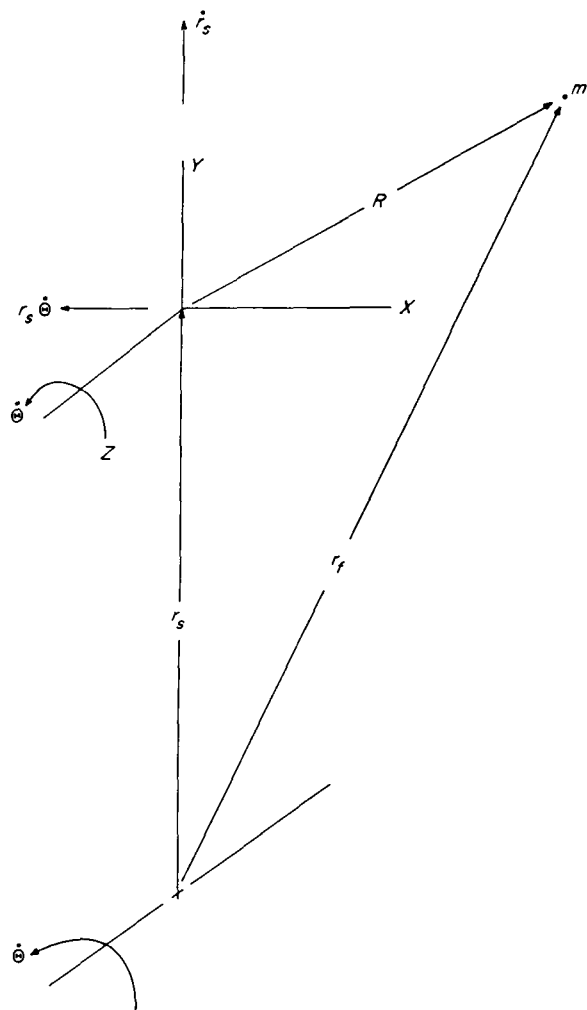
$$\mathbf{V} = \mathbf{i}[\dot{x} - (y + r_s)\dot{\Theta}] + \mathbf{j}(\dot{y} + \dot{r}_s + x\dot{\Theta}) + \mathbf{k}(\dot{z}) \quad (\text{A3})$$

The kinetic energy of the mass is then

$$\begin{aligned} T &= \frac{1}{2} m (\mathbf{V} \cdot \mathbf{V}) \\ &= \frac{1}{2} m \left\{ \dot{x}^2 + \dot{y}^2 + \dot{z}^2 + [(y + r_s)^2 + x^2] \dot{\Theta}^2 + 2\dot{y}\dot{r}_s \right. \\ &\quad \left. + \dot{r}_s^2 + 2[x(\dot{r}_s + \dot{y}) - (y + r_s)\dot{x}]\dot{\Theta} \right\} \quad (\text{A4}) \end{aligned}$$

The potential energy of the mass is given by

$$\begin{aligned} U &= -mgr_f \\ &= \frac{-mg_e r_e^2}{r_f} \\ &= -mg_e r_e^2 [x^2 + (y + r_s)^2 + z^2]^{-1/2} \quad (\text{A5}) \end{aligned}$$



Sketch 1.

notation employed. The position of the mass is given by

$$\mathbf{r}_f = \mathbf{r}_s + \mathbf{R} \quad (\text{A1})$$

With the kinetic and potential energy thus specified, the Lagrangian

$$L = T - U \quad (\text{A6})$$

can be formed and the Lagrangian operation

$$\frac{d}{dt} \left( \frac{\partial L}{\partial \dot{q}_i} \right) - \frac{\partial L}{\partial q_i} = F_i \quad (i=1, 2, 3) \quad (\text{A7})$$

performed for the equations of motion in terms of the coordinates  $x$ ,  $y$ , and  $z$  (which are  $q_1$ ,  $q_2$ , and  $q_3$  in eq. (A7)).

After the indicated operation of equation (A7) is made, the equations of motion are

$$\left. \begin{aligned} \ddot{x} - (y + r_s)\ddot{\theta} - 2(\dot{y} + \dot{r}_s)\dot{\theta} - x\dot{\theta}^2 + g_e r_e^2 \frac{x}{r_f^3} &= \frac{T_x}{m} \\ \ddot{y} + x\ddot{\theta} + 2\dot{x}\dot{\theta} + \ddot{r}_s - (y + r_s)\dot{\theta}^2 + g_e r_e^2 \frac{(y + r_s)}{r_f^3} &= \frac{T_y}{m} \\ \ddot{z} + g_e r_e^2 \frac{z}{r_f^3} &= \frac{T_z}{m} \end{aligned} \right\} \quad (\text{A8})$$

The symbols  $T_x$ ,  $T_y$ , and  $T_z$  denote the thrust forces acting on the mass in the  $x$ -,  $y$ -, and  $z$ -direction of the station coordinate system. The radial distance from the center of the gravitation field to the mass is

$$r_f = [x^2 + (y + r_s)^2 + z^2]^{1/2} \quad (\text{A9})$$

The equations which specify the variation of  $r_s$  and  $\theta$  are the Keplerian equations:

$$\left. \begin{aligned} \ddot{r}_s - r_s \dot{\theta}^2 &= -\frac{g_e r_e^2}{r_s^2} \\ r_s^2 \dot{\theta} &= C_s \end{aligned} \right\} \quad (\text{A10})$$

where  $C_s$  is the constant angular momentum of the space station. Since equations (A10) can be solved in closed form, it is normally more convenient to specify the conic section in terms of its characteristic constants and the initial position of the station. For an ellipse, one may define  $\theta = 0^\circ$  at the perigee and define the perigee  $r_{s,p}$ , the apogee  $r_{s,a}$ , and the initial position of the space station in the ellipse  $\theta_o$ . With these definitions, the following relationships can be

obtained:

the semimajor axis:

$$A = \frac{1}{2}(r_{s,p} + r_{s,a}) \quad (\text{A11})$$

the eccentricity:

$$\epsilon = \frac{r_{s,a} - r_{s,p}}{r_{s,a} + r_{s,p}} \quad (\text{A12})$$

and the angular momentum:

$$C_s = [g_e r_e^2 A(1 - \epsilon^2)]^{1/2} \quad (\text{A13})$$

Equations (A10) can then be replaced with

$$\left. \begin{aligned} t &= \frac{1}{C_s} \int_{\theta_o}^{\theta} r_s^2(\theta) d\theta \\ r_s(\theta) &= \frac{A(1 - \epsilon^2)}{1 + \epsilon \cos \theta} \end{aligned} \right\} \quad (\text{A14})$$

and the time derivatives

$$\left. \begin{aligned} \dot{r}_s &= \frac{C_s \epsilon \sin \theta}{A(1 - \epsilon^2)} \\ \ddot{r}_s &= \frac{C_s^2 \epsilon}{A(1 - \epsilon^2)} \frac{\cos \theta}{r_s^2} \\ \dot{\theta} &= \frac{C_s}{r_s^2} \\ \ddot{\theta} &= -\frac{2C_s^2 \epsilon}{A(1 - \epsilon^2)} \frac{\sin \theta}{r_s^3} \end{aligned} \right\} \quad (\text{A15})$$

For calculating the line-of-sight range between the two vehicles and the time rate of change of that range, the expressions

$$R = \sqrt{x^2 + y^2 + z^2} \quad (\text{A16})$$

$$\dot{R} = \frac{x\dot{x} + y\dot{y} + z\dot{z}}{R} \quad (\text{A17})$$

may be used.

It should be noted that the velocities measured from the rotating frame of axes in the space station are not the same as those that would be measured from the absolute frame of axes fixed at the center of the earth. As can be seen from equation

(A3), the proper relationships are

$$\left. \begin{aligned} V_x &= \dot{x} - (y + r_s) \dot{\theta} \\ V_y &= \dot{y} + \dot{r}_s + x \dot{\theta} \\ V_z &= \dot{z} \\ V^2 &= V_x^2 + V_y^2 + V_z^2 \end{aligned} \right\} \quad (\text{A18})$$

where  $V_x$ ,  $V_y$ , and  $V_z$  are the components of the inertial velocity of the ferry in the direction of the  $X$ -,  $Y$ -, and  $Z$ -axes, respectively, as measured on the nonrotating earth. Velocity components as measured by a tracking station on a rotating earth could be obtained but these are not necessary to the subject of this paper.

Two additional equations can be obtained which may prove useful if the differential equations are solved by numerical integration processes such as used by digital computers. Regardless of the orbit that is followed, if the forces are conservative (that is, aerodynamic forces and thrust are zero), the angular momentum and the total energy of the ferry vehicle must remain constant. The requirement that angular momentum be conserved requires that

$$|\mathbf{r}_f \times \mathbf{V}| = C_f = \text{Constant} \quad (\text{A19})$$

where  $\mathbf{V} = \frac{d\mathbf{r}_f}{dt}$  is given by equation (A3) and the vertical bars denote the absolute value of the resulting vector. The condition that the total energy remain constant requires that

$$T + U = E_f = \text{Constant} \quad (\text{A20})$$

Equations (A19) and (A20) are the first integrals of the motion of the ferry vehicle in terms of the coordinates of the space station. If  $C_f$  and  $E_f$  are evaluated by using the initial conditions, at any point on the trajectory the degree of accuracy of the numerical solutions may be determined by again computing either  $C_f$  or  $E_f$  and comparing the percent of change. In the case of the angular momentum, it is suggested that the vector quantities be evaluated in numerical form since the analytical expression is very cumbersome. However, for the simplified case of coplanar motion of the ferry vehicle  $z = \dot{z} = 0$ , the expression becomes simply

$$C_f = [\dot{y} + \dot{r}_s]x - [y + r_s]\dot{x} + [x^2 + (y + r_s)^2]\dot{\theta} \quad (\text{A21})$$

## APPENDIX B

### EQUATIONS OF MOTION AND APPROXIMATE SOLUTIONS TO THE MOTION OF A MASS AS MEASURED IN A ROTATING FRAME OF AXES WHICH MOVES IN A CIRCULAR ORBIT

For the case where the space station, and hence, the rotating frame of axes moves in a circular (or very nearly circular) orbit, the equations of appendix A may be simplified. If

$$\left. \begin{aligned} r_s &= \text{Constant} \\ \dot{\theta} &= \text{Constant} = \omega \end{aligned} \right\} \quad (\text{B1})$$

the differential equations (A8) become

$$\left. \begin{aligned} \ddot{x} - 2\omega\dot{y} + x\left(\frac{g_e r_e^2}{r_f^3} - \omega^2\right) &= \frac{T_x}{m} \\ \ddot{y} + 2\omega\dot{x} + (y + r_s)\left(\frac{g_e r_e^2}{r_f^3} - \omega^2\right) &= \frac{T_y}{m} \\ \ddot{z} + z\frac{g_e r_e^2}{r_f^3} &= \frac{T_z}{m} \end{aligned} \right\} \quad (\text{B2})$$

The radial distance to the ferry vehicle is defined as

$$r_f = [x^2 + (y + r_s)^2 + z^2]^{1/2} \quad (\text{B3})$$

and the orbital equations (A10) give the expression for  $\omega$  in terms of the radius  $r_s$  as

$$\omega^2 = \frac{g_e r_e^2}{r_s^3} \quad (\text{B4})$$

In these equations it is an implicit assumption that the mass of the station, the mass of the ferry vehicle, the gravitational attraction between the two masses and any other planetary bodies are all negligible compared with the mass and gravitation

field of the earth. If it is desired to go a step further and to consider cases where the ferry is never more than 100 or 200 miles from the station (in a circular orbit), very good approximate solutions can be obtained to equations (B2). The method given in reference 6 and first noted in reference 7 requires the expansion of  $r_f^{-3}$  into a power series

$$\frac{1}{r_f^3} = \frac{1}{r_s^3} \left[ 1 - 3\frac{y}{r_s} - \frac{3}{2r_s^2}(x^2 - 4y^2 + z^2) - \dots \right] \quad (\text{B5})$$

In the series, the terms of second order and higher are dropped. Substituting

$$\begin{aligned} \frac{g_e r_e^2}{r_f^3} &\approx \frac{g_e r_e^2}{r_s^3} \left( 1 - 3\frac{y}{r_s} \right) \\ &\approx \omega^2 \left( 1 - 3\frac{y}{r_s} \right) \end{aligned} \quad (\text{B6})$$

into equations (B2) and dropping the nonlinear terms containing  $y/r_s$  gives a set of linear ordinary differential equations:

$$\left. \begin{aligned} \ddot{x} - 2\omega\dot{y} &= \frac{T_x}{m} \\ \ddot{y} + 2\omega\dot{x} - 3\omega^2 y &= \frac{T_y}{m} \\ \ddot{z} + \omega^2 z &= \frac{T_z}{m} \end{aligned} \right\} \quad (\text{B7})$$

On a nonthrusting trajectory, the position and velocity of the mass at any time are given in terms of the initial conditions by the homogeneous solutions:

$$\left. \begin{aligned} x &= 2\left(2\frac{\dot{x}_o}{\omega} - 3y_o\right) \sin \omega t - 2\frac{\dot{y}_o}{\omega} \cos \omega t + \left(6y_o - 3\frac{\dot{x}_o}{\omega}\right) \omega t + x_o + 2\frac{\dot{y}_o}{\omega} \\ y &= \left(2\frac{\dot{x}_o}{\omega} - 3y_o\right) \cos \omega t + \frac{\dot{y}_o}{\omega} \sin \omega t + 4y_o - 2\frac{\dot{x}_o}{\omega} \\ z &= z_o \cos \omega t + \frac{\dot{z}_o}{\omega} \sin \omega t \end{aligned} \right\} \quad (\text{B8})$$

$$\left. \begin{aligned} \frac{\dot{x}}{\omega} &= 2 \left( 2 \frac{\dot{x}_o}{\omega} - 3y_o \right) \cos \omega t + 2 \frac{\dot{y}_o}{\omega} \sin \omega t + 6y_o - 3 \frac{\dot{x}_o}{\omega} \\ \frac{\dot{y}}{\omega} &= - \left( 2 \frac{\dot{x}_o}{\omega} - 3y_o \right) \sin \omega t + \frac{\dot{y}_o}{\omega} \cos \omega t \\ \frac{\dot{z}}{\omega} &= \frac{\dot{z}_o}{\omega} \cos \omega t - z_o \sin \omega t \end{aligned} \right\} \quad (B9)$$

It may be noted that all these quantities, with the exception of  $x$  which increases linearly with time, are periodic in time.

As a check on the numerical examples of this paper, the position and velocity of a mass (the ferry) ejected from the space station at time zero with the velocity components  $\dot{x}_o$ ,  $\dot{y}_o$ , and  $\dot{z}_o$  can be obtained at any subsequent (or prior) times by

setting  $x_o = y_o = z_o = 0$  in equations (B8) and (B9) and solving for  $x$ ,  $y$ ,  $z$ ,  $\dot{x}$ ,  $\dot{y}$ , and  $\dot{z}$  at time  $t$  (or  $-t$ ).

On the other hand, if the position of the ferry is known at any time, for example,  $t=0$ , the velocity components of the ferry relative to the space station necessary to rendezvous at some time  $\tau$  in the future can be obtained by putting equations (B8) in a slightly different form. Requiring

that  $x=y=z=0$  when  $t=\tau$  yields

$$\begin{Bmatrix} 0 \\ 0 \end{Bmatrix} = \begin{bmatrix} 4 \sin \omega \tau - 3\omega \tau & 2 - 2 \cos \omega \tau \\ 2 \cos \omega \tau - 2 & \sin \omega \tau \end{bmatrix} \begin{Bmatrix} \frac{\dot{x}_o}{\omega} \\ \frac{\dot{y}_o}{\omega} \end{Bmatrix} + \begin{bmatrix} 1 & 6\omega \tau - 6 \sin \omega \tau \\ 0 & 4 - 3 \cos \omega \tau \end{bmatrix} \begin{Bmatrix} x_o \\ y_o \end{Bmatrix}$$

$$0 = z_o \cos \omega \tau + \frac{\dot{z}_o}{\omega} \sin \omega \tau$$

where

$$\Delta = 3\omega \tau \sin \omega \tau - 8(1 - \cos \omega \tau)$$

Solving for the velocities in terms of the displacements gives

$$\left. \begin{aligned} \frac{\dot{x}_o}{\omega} &= \frac{x_o \sin \omega \tau + y_o [6\omega \tau \sin \omega \tau - 14(1 - \cos \omega \tau)]}{\Delta} \\ \frac{\dot{y}_o}{\omega} &= \frac{2x_o (1 - \cos \omega \tau) + y_o (4 \sin \omega \tau - 3\omega \tau \cos \omega \tau)}{\Delta} \\ \frac{\dot{z}_o}{\omega} &= \frac{-z_o}{\tan \omega \tau} \end{aligned} \right\} \quad (B10)$$

Again, it should be noted that the velocity components of the ferry as measured from the space station are not the same as the components measured from a nonrotating earth. The proper relationships are obtained from equation (A3) as

$$\left. \begin{aligned} V_x &= \dot{x} - (y + r_s) \omega \\ V_y &= \dot{y} + x \omega \\ V_z &= \dot{z} \\ V^2 &= V_x^2 + V_y^2 + V_z^2 \end{aligned} \right\} \quad (B11)$$

## APPENDIX C

### POSITION AND VELOCITY OF FERRY WITH RESPECT TO EARTH-FIXED COORDINATE SYSTEM

The position of the ferry vehicle as seen from the center of the earth will be defined with the spherical coordinates  $r_f$ ,  $\Delta\theta$ , and  $\zeta$  as shown in sketch 2. The angle  $\Delta\theta$  lies in the orbital plane of the station and the angle  $\zeta$  is measured normal

to the orbital plane. In terms of coordinates of the space station, these earth-measured coordinates are defined by

$$\left. \begin{aligned} \Delta\theta &= \tan^{-1} \frac{x}{y+r_s} & (0 \leq \Delta\theta < 2\pi) \\ \zeta &= \tan^{-1} \frac{z}{[x^2 + (y+r_s)^2]^{1/2}} & (-\pi < \zeta \leq \pi) \\ r_f &= [x^2 + (y+r_s)^2 + z^2]^{1/2} \end{aligned} \right\} \quad (C1)$$

The velocity components of the ferry as measured in a Cartesian frame of axes fixed at the center of the earth were given by equations (A18) and (B11) for the two classes of orbits considered. If these velocity components are rotated first through the angle  $\Delta\theta$  and then through the angle  $\zeta$ , the spherical velocity components are given by

$$\left. \begin{aligned} V_r &= \dot{r}_f = (V_x \sin \Delta\theta + V_y \cos \Delta\theta) \cos \zeta + V_z \sin \zeta \\ V_\zeta &= r_f \dot{\zeta} = -(V_x \sin \Delta\theta + V_y \cos \Delta\theta) \sin \zeta + V_z \cos \zeta \\ V_\theta &= r_f \cos \zeta \dot{\Delta\theta} = V_x \cos \Delta\theta - V_y \sin \Delta\theta \end{aligned} \right\} \quad (C2)$$

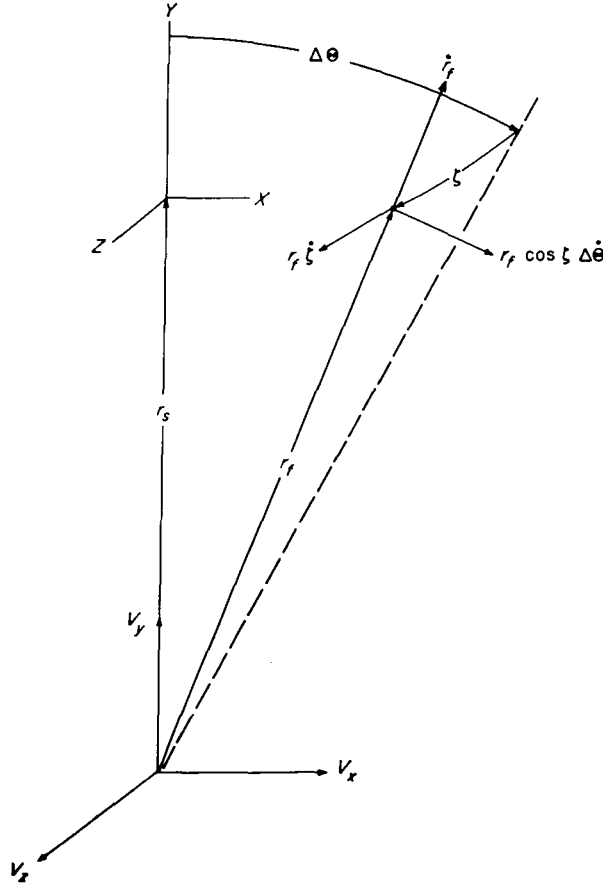
and are shown in sketch 2.

The velocity components  $V_\zeta$  and  $V_\theta$  define the plane of the local horizontal and the total tangential (horizontal) component of the velocity is

$$V_t = \sqrt{V_\zeta^2 + V_\theta^2} \quad (C3)$$

and makes an angle

$$\eta_f = \tan^{-1} \frac{V_\zeta}{V_\theta} \quad (C4)$$



Sketch 2.

with the plane of the station's orbit. The local flight-path angle is defined as the angle between the resultant velocity vector and the local horizon and is given by

$$\gamma_f = \tan^{-1} \frac{V_r}{V_t} \quad (C5)$$

It should be noted that the in-plane angular position of the ferry with respect to the reference position  $\theta=0$  is given by the angle  $\theta - \Delta\theta = \theta_f$ .



## APPENDIX D

### ANALYTICAL CALCULATION OF BOUNDARIES OF LAUNCH AND RENDEZVOUS CONDITIONS

The boundaries of launch and rendezvous conditions, given in figure 12 for a circular orbit and in figure 19 for an elliptic orbit, can be calculated analytically from relatively simple considerations. Since the procedure for calculating the boundaries is the same for either type of orbit, the equations are given for the more general case of the station in an elliptic orbit. The simplifications obtained with the station in a circular orbit will then be noted.

For a specified orbit of the station where rendezvous is to occur at the angular position  $\Theta$ , the conditions at that position are given by

$$r_s = \frac{A(1-\epsilon^2)}{1+\epsilon \cos \Theta} \quad (D1)$$

$$V_s^2 = 2g_e r_e^2 \left( \frac{1}{r_s} - \frac{1}{2A} \right) \quad (D2)$$

$$\tan \gamma_s = \frac{\dot{r}_s}{r_s \dot{\Theta}} = \frac{\epsilon \sin \Theta}{1+\epsilon \cos \Theta} \quad (D3)$$

The expressions for  $A$  and  $\epsilon$  are given in appendix A. (See eqs. (A11) and (A12).)

In order to obtain the  $\gamma_L=0^\circ$  boundaries for rendezvous at the specified position of the station, the perigee of the ferry trajectory is held fixed at the launch altitude so that

$$r_{f,p} = r_L = 60 + 3,960 = 4,020 \text{ miles}$$

and the apogee radius  $r_{f,a}$  is varied from the radius of the station  $r_s$  over a range of values greater than  $r_s$ . For each value of  $r_{f,a}$  that is chosen, the associated launch conditions are

$$V_L^2 = V_{f,p}^2 = 2g_e r_e^2 \left( \frac{1}{r_{f,p}} - \frac{1}{r_{f,p} + r_{f,a}} \right) \quad (D4)$$

$$\gamma_L = 0 \quad (D5)$$

The velocity and flight-path angle of the ferry at

rendezvous are obtained at the condition  $r_f = r_s$ ; therefore,

$$V_f^2 = 2g_e r_e^2 \left( \frac{1}{r_s} - \frac{1}{r_{f,p} + r_{f,a}} \right) \quad (D6)$$

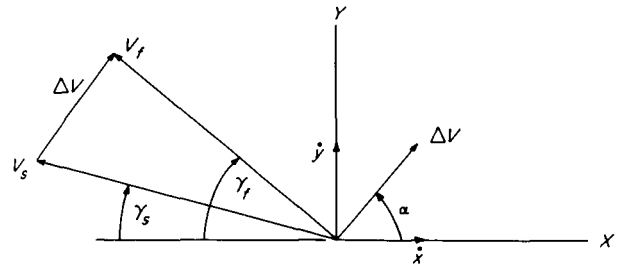
$$\cos \gamma_f = \frac{r_{f,p}}{r_{f,a}} \frac{V_{f,p}}{V_{f,a}} \quad (D7)$$

The relative velocity components are computed from the relations

$$\dot{x} = V_s \cos \gamma_s - V_f \cos \gamma_f$$

$$\dot{y} = V_f \sin \gamma_f - V_s \sin \gamma_s$$

The situation is shown in sketch 3. Note that



Sketch 3.

only coplanar motion is considered here; therefore, with  $\beta=0$ ,  $\Delta V$  is used instead of  $\Delta V \cos \beta$ . The velocity and angle of closure are then obtained from the relations

$$\begin{aligned} \Delta V^2 &= \dot{x}^2 + \dot{y}^2 \\ &= V_s^2 + V_f^2 - 2V_s V_f \cos (\gamma_f - \gamma_s) \end{aligned} \quad (D8)$$

$$\begin{aligned} \tan \alpha &= \frac{\dot{y}}{\dot{x}} \\ &= \frac{V_f \sin \gamma_f - V_s \sin \gamma_s}{V_s \cos \gamma_s - V_f \cos \gamma_f} \end{aligned} \quad (D9)$$

Thus, equations (D1) to (D3) give the station conditions at rendezvous; equations (D4) and (D5)

give the ferry launch conditions; equations (D6) and (D7) give the ferry rendezvous conditions; and equations (D8) and (D9) give the relative conditions at rendezvous.

The constant  $\Delta V$  boundaries are obtained by following the procedure in reverse. By holding  $\Delta V$  constant and varying  $\alpha$ , one obtains

$$V_f^2 = V_s^2 + \Delta V^2 - 2V_s \Delta V \cos(\alpha + \gamma_s) \quad (\text{D10})$$

$$\tan \gamma_f = \frac{V_s \sin \gamma_s + \Delta V \sin \alpha}{V_s \cos \gamma_s - \Delta V \cos \alpha} \quad (\text{D11})$$

Without calculating the perigee or apogee of the transfer ellipse, the conditions at ferry launch are obtained from the expressions of constant total energy and constant angular momentum:

$$V_L^2 = V_f^2 - 2g_e r_e^2 \left( \frac{1}{r_L} - \frac{1}{r_s} \right) \quad (\text{D12})$$

$$\cos \gamma_L = \frac{r_s}{r_L} \frac{V_s \cos \gamma_s - \Delta V \cos \alpha}{V_L} \quad (\text{D13})$$

Thus,  $\Delta V$  and  $\alpha$  are specified; equations (D10) and (D11) give the ferry conditions at rendezvous; and equations (D12) and (D13) give the ferry conditions at launch. This procedure may also be followed for contours of constant  $\alpha$  and variable  $\Delta V$ .

Extreme caution should be exercised in the use of equations (D10) to (D13). When  $\Delta V$  is close to its minimum possible value and also when  $\gamma_L$  approaches  $0^\circ$ , the equations become particularly sensitive to small computational errors.

When the station's orbit is circular, all the above equations still hold with the simplifications that

$$\gamma_s = 0 \quad (\text{D14})$$

since

$$\epsilon = 0$$

$$r_s = A$$

$$V_s^2 = \frac{g_e r_e^2}{r_s} = V_c^2$$

and the absolute value of  $\theta$  at the time of rendezvous is no longer relevant.

#### REFERENCES

1. Houbolt, John C.: Considerations of the Rendezvous Problems for Space Vehicles. Preprint No. 175A, Soc. Automotive Eng., Apr. 1960.
2. Bird, John D., and Thomas, David F., Jr.: A Two-Impulse Plan for Performing Rendezvous on a Once-a-Day Basis. NASA TN D-437, 1960.
3. Swanson, Robert S., and Petersen, Norman V.: The Influence of Launch Conditions on the Friendly Rendezvous of Astrovehicles. Preprint No. 59-16, Am. Astronautical Soc., Aug. 1959.
4. Petersen, Norman V., and Swanson, Robert S.: Rendezvous in Space—Effects of Launch Conditions. Proc. Manned Space Stations Symposium, Inst. Aero. Sci., c.1960.
5. Martin, B. P.: Dual Burning Propulsion Systems for Satellite Stages. Jour. Astronautical Sci., vol. VII, no. 1, Spring 1960, pp. 21-23.
6. Clohessy, W. H., and Wiltshire, R. S.: Terminal Guidance System for Satellite Rendezvous. Preprint No. 59-93, S.M.F. Fund Paper, Inst. Aero. Sci., June 1959.
7. Wheelon, Albert D.: An Introduction to Midcourse and Terminal Guidance. GM-TM-0165-00252, Space Tech. Labs., June 10, 1958.